**Electronic Supplementary Information**

# Iridium and rhodium complexes bearing a silyl–bipyridine pincer ligand: synthesis, structures and catalytic activity for C–H borylation of arenes

Takashi Komuro,* Daiki Mochizuki, Hisako Hashimoto* and Hiromi Tobita

*Department of Chemistry, Graduate School of Science, Tohoku University, Sendai 980-8578, Japan.*

*E-mail: takashi.komuro.c5@tohoku.ac.jp (T.K.); hisako.hashimoto.b7@tohoku.ac.jp (H.H.)*

## Contents

## 1. Experimental procedures and characterisation data

**General considerations.** All manipulations, except purification of the ligand precursor $Bpy^{SiNN}(H)$, were performed under dry argon in a glovebox or using a high-vacuum line and standard Schlenk techniques. Glassware was dried under vacuum prior to use. Purification of $Bpy^{SiNN}(H)$ was performed in the air.

**Materials.** Benzene-$d_6$ ($C_6D_6$, 99.6%D), tetrahydrofuran-$d_8$ (THF-$d_8$), $CDCl_3$, toluene, pinacolborane, fluorobenzene and bromobenzene were dried over $CaH_2$ and vacuum-transferred, and then stored under argon over 4 Å molecular sieves in a glovebox. THF and hexane were dried using a Glass Contour alumina column (Nikko Hansen & Co., Ltd), degassed by three freeze-pump-thaw cycles and then stored under argon over 4 Å molecular sieves in a glovebox. Trimethylphosphine ($PMe_3$) and bis(pinacolato)diboron ($B_2pin_2$) were purchased and stored in a glovebox at –35 °C (for $PMe_3$) or room temperature (for $B_2pin_2$). 6-Methyl-2,2´-bipyridine,[S1] ($t$-Bu)$_2$Si(H)Cl,[S2] $[IrCl(cod)]_2$,[S3] $[RhCl(coe)_2]_2$[S4] and an iridium complex bearing a 2,6-lutidine-based silyl–pyridine–amine pincer ligand ($Lut^{SiNN}$), $Ir(Lut^{SiNN})(H)Cl$ (**A**),[S5] were prepared according to previously reported method.

**Spectroscopic measurements.** $^{1}H$, $^{11}B$, $^{11}B\{^{1}H\}$, $^{13}C\{^{1}H\}$, $^{19}F\{^{1}H\}$, $^{29}Si\{^{1}H\}$ and $^{31}P\{^{1}H\}$ NMR spectra were recorded on a Bruker AVANCE III 400 Fourier transform spectrometer. Chemical shifts are reported in parts per million (ppm), and coupling constants ($J$) and line widths at half-height ($\Delta\nu_{1/2}$) are given in Hz. $^{29}Si\{^{1}H\}$ NMR measurements were performed using a DEPT or inverse gate decoupling (IG) pulse sequence. The residual proton ($C_6D_5H$, 7.15 ppm; $CHCl_3$, 7.24 ppm; THF-$d_7$, 3.58 ppm) and the carbon ($C_6D_6$, 128.0 ppm; $CDCl_3$, 77.0 ppm; THF-$d_8$, 67.4 ppm) resonances of deuterated solvents were used as internal references for $^{1}H$ and $^{13}C$ resonances, respectively. Aromatic protons, aromatic carbons, bipyridine protons and bipyridine carbons are abbreviated as Ar-H, Ar-C, bpy-H and bpy-C, respectively. $^{11}B$, $^{19}F\{^{1}H\}$, $^{29}Si\{^{1}H\}$ and $^{31}P\{^{1}H\}$ NMR chemical shifts were referenced to $BF_3$•$Et_2O$ (0 ppm), $C_6H_5CF_3$ (–63.7 ppm),

$SiMe_4$ (0 ppm) and 85% $H_3PO_4$ (0 ppm), respectively, as external standards. NMR data were collected at room temperature unless otherwise indicated. Infrared spectra were recorded for solid samples in KBr pellets, or for neat samples placed between KBr plates using a Horiba FT-720 spectrometer. High-resolution mass spectra (HRMS) and mass spectra were recorded on a Bruker Daltonics solariX 9.4T spectrometer operating in electrospray ionization (ESI) mode or on a JEOL JMS-T100GCV spectrometer operating in field desorption (FD) mode. Elemental analyses were performed using a J-Science Lab JM11 microanalyzer. Mass spectroscopic measurements and elemental analyses were performed at the Research and Analytical Center for Giant Molecules, Tohoku University.

**1.1 Synthesis of 6-(di-*tert*-butylsilyl)methyl-2,2´-bipyridine [Bpy$^{SiNN}$(H)].**

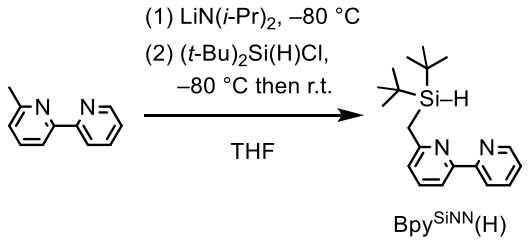

Bpy$^{SiNN}$(H)

In a 500 mL round-bottomed flask, diisopropylamine (4.5 mL, $d$ = 0.72 g mL$^{-1}$, 32 mmol) was dissolved in THF (50 mL). The solution was cooled using an ice bath, and then to the solution was added dropwise *n*-BuLi (22.2 mL, 1.58 M in hexane, 35.1 mmol) with stirring. After the solution was stirred for 15 min at 0 °C, the resulting solution involving LiN(*i*-Pr)$_2$ was cooled at ca. –80 °C using a MeOH/liq. $N_2$ bath. A solution of 6-methyl-2,2´-bipyridine (5.10 g, 30.0 mmol) in THF (40 mL) was added slowly to the solution. The colour of the reaction mixture was changed from colourless to deep green. After the solution was stirred for 1 h at ca. –80 °C, di-*tert*-butyl(chloro)silane (8.1 mL, $d$ = 0.88 g mL$^{-1}$, 40 mmol) was added dropwise to the solution. The mixture was warmed to room temperature and then was stirred at room temperature for a further 2 h. The reaction was quenched by treatment with a saturated $NaHCO_3$ solution (100 mL). Yellow organic phase

was collected, and aqueous phase was further extracted with $Et_2O$ (50 mL × 2). The organic phase was combined, washed with saturated brine (100 mL) and then dried over $MgSO_4$. After filtration, volatiles were removed from the filtrate under vacuum. Yellow volatile impurities involving in the residual orange oil were removed by Kugelrohr distillation (2 Pa, 150 °C). The residual colourless liquid was solidified after several hours at room temperature. The title compound was obtained as a colourless solid (9.076 g, 28.9 mmol) in 97% yield.

$^1$H NMR (400 MHz, r.t., $C_6D_6$): $\delta$ 1.01 [s, 18H, Si{C($CH_3$)$_3$}$_2$], 2.50 (d, 2H, $^3J_{HH}$ = 3.2 Hz, $SiCH_2$), 3.79 (t with satellites, 1H, $^3J_{HH}$ = 3.2 Hz, $^1J_{SiH}$ = 185 Hz, Si–H), 6.74 (ddd, 1H, $^3J_{HH}$ = 7.8 Hz, $^4J_{HH}$ = 4.7 Hz, $^4J_{HH}$ = 1.0 Hz, bpy-H$^{5'}$), 6.83 (dd, 1H, $^3J_{HH}$ = 7.7 Hz, $^4J_{HH}$ = 0.8 Hz, bpy-H$^5$), 7.26 (t, 1H, $^3J_{HH}$ = 7.7 Hz, bpy-H$^4$), 7.30 (td, 1H, $^3J_{HH}$ = 7.8 Hz, $^4J_{HH}$ = 1.8 Hz, bpy-H$^{4'}$), 8.49 (dd, 1H, $^3J_{HH}$ = 7.7 Hz, $^4J_{HH}$ = 0.8 Hz, bpy-H$^3$), 8.53 (ddd, 1H, $^3J_{HH}$ = 4.7 Hz, $^4J_{HH}$ = 1.8 Hz, $^5J_{HH}$ = 1.0 Hz, bpy-H$^{6'}$), 8.68 (dt, 1H, $^3J_{HH}$ = 7.8 Hz, $^4J_{HH}$ = $^5J_{HH}$ = 1.0 Hz, bpy-H$^{3'}$).[S6] $^{13}$C{$^1$H} NMR (101 MHz, r.t., $C_6D_6$): $\delta$ 19.4 [Si{*C*($CH_3$)$_3$}$_2$], 22.7 ($SiCH_2$), 29.0 [Si{C(*C*$H_3$)$_3$}$_2$], 117.2 (bpy-C$^3$), 120.9 (bpy-C$^{3'}$), 123.1 (bpy-C$^5$), 123.4 (bpy-C$^{5'}$), 136.4 (bpy-C$^{4'}$), 136.9 (bpy-C$^4$), 149.3 (bpy-C$^{6'}$), 155.7 (bpy-C$^2$), 157.0 (bpy-C$^{2'}$), 161.4 (bpy-C$^6$).[S6] $^{29}$Si{$^1$H} NMR (79.5 MHz, DEPT, r.t., $C_6D_6$): $\delta$ 14.6. IR (KBr-pellet, cm$^{-1}$): 2112 (s, $\nu_{Si–H}$). HRMS (ESI, positive, additive: $CH_3COOH$): *m*/*z* calcd for [$C_{19}H_{28}N_2Si$ + H]$^+$ ([M + H]$^+$) 313.2095, found 313.2096. Anal. Calcd for $C_{19}H_{28}N_2Si$: C, 73.02; H, 9.03; N, 8.96. Found: C, 73.01; H, 9.03; N, 9.14.

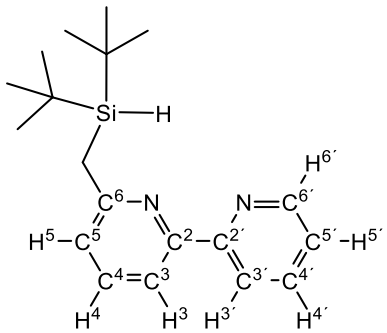

**1.2 Synthesis of Ir(Bpy$^{SiNN}$)(H)Cl (1).**

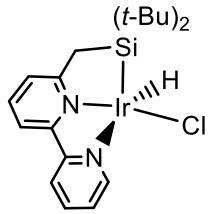


**1**

In a 30 mL Schlenk tube, Bpy$^{SiNN}$(H) (211 mg, 0.675 mmol) and [IrCl(cod)]$_2$ (200 mg, 0.298 mmol; 0.44 equiv.) were dissolved in toluene (12 mL). After the orange solution was stirred at room temperature for 16 h, the resulting dark green solution was evaporated under vacuum. The residue was extracted with THF, and the extract was filtered through a syringe filter. The filtrate was then concentrated under vacuum, leading to the precipitation of a dark green solid. This solid was collected by filtration and dried under vacuum. Ir(Bpy$^{SiNN}$)(H)Cl (**1**) was obtained as a dark green powder (215 mg, 0.398 mmol) in 67% yield.

$^1$H NMR (400 MHz, r.t., $C_6D_6$): $\delta$ −17.94 (s, 1H, Ir−H), 1.27 [br s, 18H, Si{C($CH_3$)$_3$}$_2$], 1.98 (br s, 2H, $SiCH_2$), 6.50 (br d, 1H, $^3J_{HH}$ = 7.6 Hz, bpy-H), 6.54 (br d, 1H, $^3J_{HH}$ = 7.6 Hz, bpy-H), 6.60 (dt, 1H, $^3J_{HH}$ = 5.2 Hz, $^4J_{HH}$ = 3.1 Hz, bpy-H), 6.83−6.89 (m, 2H, bpy-H), 7.17 (d, 1H, $^3J_{HH}$ = 7.8 Hz, bpy-H), 9.56 (br d, 1H, $^4J_{HH}$ = 5.2 Hz, bpy-H). $^1$H NMR (400 MHz, r.t., THF-$d_8$): $\delta$ −19.18 (s, 1H, Ir−H), 0.97 [br s, $\Delta\nu_{1/2}$ = 8.4 Hz, 18H, Si($t$-Bu)$_2$], 2.14 (br s, $\Delta\nu_{1/2}$ = 15.6 Hz, 2H, $SiCH_2$), 7.23 (dd, 1H, $^3J_{HH}$ = 7.8 Hz, $^4J_{HH}$ = 0.9 Hz, bpy-H$^5$), 7.78 (d, 1H, $^3J_{HH}$ = 7.8 Hz, bpy-H$^3$), 7.83 (ddd, 1H, $^3J_{HH}$ = 7.8 Hz, $^3J_{HH}$ = 5.4 Hz, $^4J_{HH}$ = 1.2 Hz, bpy-H$^{5'}$), 7.99 (t, 1H, $^3J_{HH}$ = 7.8 Hz, bpy-H$^4$), 8.24 (td, 1H, $^3J_{HH}$ = 7.8 Hz, $^4J_{HH}$ = 1.7 Hz, bpy-H$^{4'}$), 8.36 (d, 1H, $^3J_{HH}$ = 7.8 Hz, bpy-H$^{3'}$), 9.44 (ddd, 1H, $^3J_{HH}$ = 5.4 Hz, $^4J_{HH}$ = 1.7 Hz, $^5J_{HH}$ = 0.7 Hz, bpy-H$^{6'}$).[S6] $^{13}$C{$^1$H} NMR (101 MHz, r.t., THF-$d_8$): $\delta$ 22.9 [Si{$C$($CH_3$)$_3$}$_2$], 30.2 [Si{C($C$H$_3$)$_3$}$_2$], 34.7 ($SiCH_2$), 121.2 (bpy-C$^3$), 122.9 (bpy-C$^{3'}$), 124.7 (bpy-C$^5$), 126.0 (bpy-C$^{5'}$), 132.7 (bpy-C$^4$), 140.7 (bpy-C$^{4'}$), 149.8 (bpy-C$^{6'}$), 157.9 (bpy-C$^2$), 161.7 (bpy-C$^{2'}$), 169.6 (bpy-C$^6$).[S6] $^{29}$Si{$^1$H} NMR (79.5 MHz, r.t., IG, THF-$d_8$): $\delta$ 32.9. IR (KBr pellet,

cm$^{-1}$): 2256 (w, $\nu_{Ir-H}$). HRMS (FD, positive): *m*/*z* calcd for [$^{12}C_{19}{}^{1}H_{28}{}^{14}N_2{}^{28}Si^{35}Cl^{193}Ir$]$^+$ ([M]$^+$) 540.1334, found 540.1335. Anal. Calcd for $C_{19}H_{28}N_2SiClIr$: C, 42.25; H, 5.22; N, 5.19. Found: C, 42.11; H, 5.23; N, 5.14.

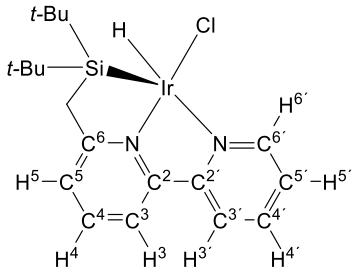


### 1.3 Variable-temperature $^1$H NMR experiments of Ir(Bpy$^{SiNN}$)(H)Cl (1)

In a Pyrex NMR tube (5 mm o.d.) fitted with a ground-glass joint, **1** was dissolved in THF-$d_8$ (0.4 mL). The NMR tube was connected to a vacuum line, and the solution was degassed by a freeze-pump-thaw cycle. The tube was then flame-sealed under vacuum. Variable-temperature $^1$H NMR spectra of the sample were recorded in the temperature range from 313 to 213 K. The spectra at 313, 300, 273, 263, 253 and 213 K are depicted in Fig. S9 (page S27), and the spectroscopic data at 313, 300 and 213 K are indicated below.

$^1$H NMR (400 MHz, 313 K, THF-$d_8$): $\delta$ −19.15 (s, 1H, Ir−H), 0.98 [br s, 18H, $\Delta\nu_{1/2}$ = 4.4 Hz, Si(*t*-Bu)$_2$], 2.15 (br s, 2H, $\Delta\nu_{1/2}$ = 7.5 Hz, SiCH$_2$), 7.23 (dd, 1H, $^3J_{HH}$ = 7.6 Hz, $^4J_{HH}$ = 0.8 Hz, bpy-H$^5$), 7.76 (d, 1H, $^3J_{HH}$ = 7.6 Hz, bpy-H$^3$), 7.82 (ddd, 1H, $^3J_{HH}$ = 8.0 Hz, $^3J_{HH}$ = 5.4 Hz, $^4J_{HH}$ = 1.1 Hz, bpy-H$^{5'}$), 7.98 (t, 1H, $^3J_{HH}$ = 7.6 Hz, bpy-H$^4$), 8.23 (td, 1H, $^3J_{HH}$ = 8.0 Hz, $^4J_{HH}$ = 1.7 Hz, bpy-H$^{4'}$), 8.34 (d, 1H, $^3J_{HH}$ = 8.0 Hz, bpy-H$^{3'}$), 9.45 (ddd, 1H, $^3J_{HH}$ = 5.4 Hz, $^4J_{HH}$ = 1.7 Hz, $^5J_{HH}$ = 0.8 Hz, bpy-H$^{6'}$).

$^1$H NMR (400 MHz, 300 K, THF-$d_8$): $\delta$ −19.19 (s, 1H, Ir−H), 0.97 [br s, 18H, $\Delta\nu_{1/2}$ = 8.4 Hz, Si(*t*-Bu)$_2$], 2.14 (br s, 2H, $\Delta\nu_{1/2}$ = 15.6 Hz, SiCH$_2$), 7.23 (dd, 1H, $^3J_{HH}$ = 7.8 Hz, $^4J_{HH}$ = 0.9 Hz, bpy-H$^5$), 7.78 (d, 1H, $^3J_{HH}$ = 7.8 Hz, bpy-H$^3$), 7.83 (ddd, 1H, $^3J_{HH}$ = 7.8 Hz, $^3J_{HH}$ = 5.4 Hz, $^4J_{HH}$ = 1.2 Hz, bpy-H$^{5'}$), 7.99 (t, 1H, $^3J_{HH}$ = 7.8 Hz, bpy-H$^4$), 8.24 (td, 1H, $^3J_{HH}$ =

7.8 Hz, $^4J_{HH}$ = 1.7 Hz, bpy-H$^{4'}$), 8.36 (d, 1H, $^3J_{HH}$ = 7.8 Hz, bpy-H$^{3'}$), 9.44 (d, 1H, $^3J_{HH}$ = 5.4 Hz, $^4J_{HH}$ = 1.7 Hz, $^5J_{HH}$ = 0.7 Hz, bpy-H$^{6'}$).

$^1$H NMR (400 MHz, 213 K, THF-$d_8$): $\delta$ −20.84 (br s, 1H, Ir−H), 0.70 [s, 9H, Si(*t*-Bu)], 1.09 [s, 9H, Si(*t*-Bu)], 1.81 (d, 1H, $^2J_{HH}$ = 16.4 Hz, $SiCH_2$), 2.30 (d, 1H, $^2J_{HH}$ = 16.4 Hz, $SiCH_2$), 7.31 (br d, 1H, $^3J_{HH}$ = 7.4 Hz, bpy-H$^5$), 7.88 (br dd, 1H, $^3J_{HH}$ = ca. 8 Hz, $^3J_{HH}$ = ca. 5 Hz, bpy-H$^{5'}$), 7.93–7.97 (m, 1H, bpy-H$^3$), 7.97–8.02 (m, 1H, bpy-H$^4$), 8.30 (br td, 1H, $^3J_{HH}$ = 8.0 Hz, $^4J_{HH}$ = 1.3 Hz, bpy-H$^{4'}$), 8.49 (d, 1H, $^3J_{HH}$ = 8.0 Hz, bpy-H$^{3'}$), 9.34 (br d, 1H, $^3J_{HH}$ = 5.1 Hz, bpy-H$^{6'}$).

### 1.4 Synthesis of Rh(Bpy$^{SiNN}$)(H)Cl (2).

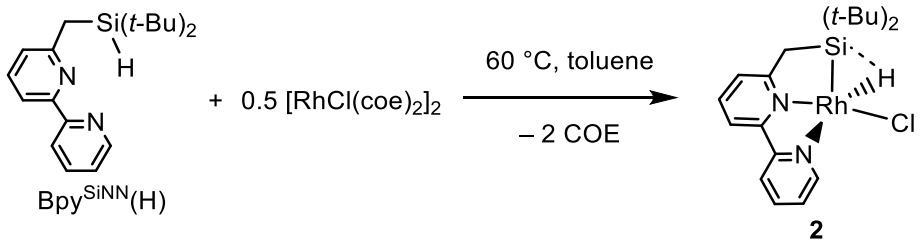


A 30 mL reaction tube fitted with J-Young Teflon valve was charged with Bpy$^{SiNN}$(H) (150 mg, 0.480 mmol) and $[RhCl(coe)]_2$ (165 mg, 0.230 mmol; 0.48 equiv.), and the reactants were suspended in toluene (8 mL). After the yellow suspension was heated at 60 °C for 45 min, the resulting dark red suspension was evaporated under vacuum. The residue was washed with $Et_2O$ (ca. 1 mL × 3) and hexane (ca. 1 mL × 3) in this order, followed by being dried under vacuum. Rh(Bpy$^{SiNN}$)(H)Cl (**2**) was obtained as a red powder (182 mg, 0.404 mmol) in 91% yield.

$^1$H NMR (400 MHz, r.t., $C_6D_6$): $\delta$ −16.00 (br d with satellites, 1H, $^1J_{RhH}$ = 29.8 Hz, $J_{SiH}$ = 33 Hz, Rh−H), 1.40 [s, 18H, Si(*t*-Bu)$_2$], 2.14 (br s, 2H, $SiCH_2$), 6.47 (ddd, 1H, $^3J_{HH}$ = 7.5 Hz, $^3J_{HH}$ = 5.4 Hz, $^4J_{HH}$ = 0.9 Hz, bpy-H), 6.55 (br d, 1H, $^3J_{HH}$ = 7.7 Hz, bpy-H), 6.67 (br d, 1H, $^3J_{HH}$ = 7.5 Hz, bpy-H), 6.83 (dt, 1H, $^3J_{HH}$ = 7.8 Hz, $^4J_{HH}$ = 1.7 Hz, bpy-H), 6.84 (t, 1H, $^3J_{HH}$ = 7.7 Hz, bpy-H), 6.92 (br d, 1H, $^3J_{HH}$ = 8.0 Hz, bpy-H), 9.40 (br dd, 1H, $^3J_{HH}$ = 5.4

Hz, $^4J_{HH}$ = 0.9 Hz, bpy-H). $^1$H NMR (400 MHz, r.t., THF-$d_8$): $\delta$ −16.74 (br d with satellites, 1H, $^1J_{RhH}$ = 29.8 Hz, $J_{SiH}$ = 39 Hz, Rh−H), 1.13 [s, 18H, Si(*t*-Bu)$_2$], 2.40 (br s, 2H, SiCH$_2$), 7.37 (d, 1H, $^3J_{HH}$ = 7.8 Hz, bpy-H$^5$), 7.66 (ddd, 1H, $^3J_{HH}$ = 7.9 Hz, $^3J_{HH}$ = 5.3 Hz, $^4J_{HH}$ = 1.1 Hz, bpy-H$^{5'}$), 7.77 (t, 1H, $^3J_{HH}$ = 7.8 Hz, bpy-H$^4$), 7.94 (d, 1H, $^3J_{HH}$ = 7.8 Hz, bpy-H$^3$), 8.13 (dt, 1H, $^3J_{HH}$ = 7.9 Hz, $^4J_{HH}$ = 1.6 Hz, bpy-H$^{4'}$), 8.45 (d, 1H, $^3J_{HH}$ = 7.9 Hz, bpy-H$^{3'}$), 9.23 (br dd, 1H, $^3J_{HH}$ = 5.3 Hz, $^5J_{HH}$ = 0.7 Hz, bpy-H$^{6'}$).[S6] $^{13}$C{$^1$H} NMR (101 MHz, r.t., THF-$d_8$): $\delta$ 24.3 [Si{*C*(CH$_3$)$_3$}$_2$], 30.8 [Si{C(*C*H$_3$)$_3$}$_2$], 32.3 (d, $^2J_{RhC}$ = 2.5 Hz, SiCH$_2$), 120.2 (bpy-C$^3$), 122.5 (bpy-C$^{3'}$), 125.0 (bpy-C$^5$), 126.1 (bpy-C$^{5'}$), 135.1 (bpy-C$^4$), 140.3 (bpy-C$^{4'}$), 150.2 (bpy-C$^{6'}$), 156.3 (bpy-C$^2$), 158.2 (bpy-C$^{2'}$), 167.7 (bpy-C$^6$).[S6] $^{29}$Si{$^1$H} NMR (79.5 MHz, r.t., IG, THF-$d_8$): $\delta$ 58.3 (d, $^1J_{RhSi}$ = 26.5 Hz). IR (KBr pellet, cm$^{-1}$): 2141 (w, $\nu_{Rh–H}$). HRMS (ESI, positive, additive: NaI): *m*/*z* calcd for [$^{12}$C$_{19}$$^1$H$_{28}$$^{14}$N$_2$$^{28}$Si$^{35}$Cl$^{103}$Rh + $^{23}$Na]$^+$ ([M + Na]$^+$) 473.0658, found 473.0657. Anal. Calcd for C$_{19}$H$_{28}$N$_2$SiClRh: C, 50.61; H, 6.26; N, 6.21. Found: C, 50.73; H, 6.34; N, 6.28.

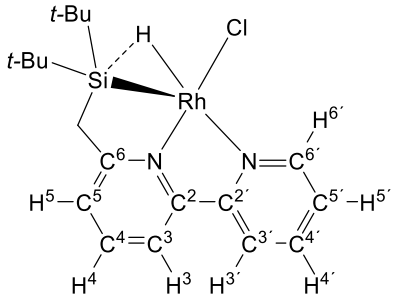


**1.5 Synthesis of Ir(Bpy$^{SiNN}$)(H)(PMe$_3$)Cl (3).**

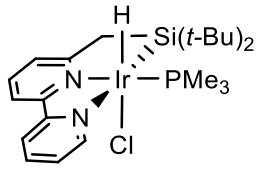


**3**

In a 15 mL Schlenk tube, to a dark-green solution of Ir(Bpy$^{SiNN}$)(H)Cl (**1**) (54 mg, 0.10 mmol) in THF (5 mL) was added trimethylphosphine (PMe$_3$) (11.2 mL, $d$ = 0.748 g mL$^{-1}$, 0.11 mmol). The colour of the solution was immediately changed to orange. After the

orange solution was evaporated under vacuum, the residue was dissolved in a minimum amount of $CH_2Cl_2$. Hexane was layered on the top of the $CH_2Cl_2$ solution and allowed to be diffused into the solution at room temperature. After several days, reddish orange crystals were precipitated. The mother liquor was removed, and the crystals were dried under vacuum. The first crop of Ir(Bpy$^{SiNN}$)(H)($PMe_3$)Cl (**3**) was obtained as reddish-orange crystals (55 mg). The mother liquor was evaporated under vacuum, and the residue was recrystalized from hexane/$CH_2Cl_2$. The second crop of complex **3** (2 mg) was then obtained. Total yield of **3**: 57 mg, 0.092 mmol; 92%.

$^1$H NMR (400 MHz, r.t., $CD_2Cl_2$): $\delta$ –23.73 (d with satellites, 1H, $^2J_{PH}$ = 22.8 Hz, $J_{SiH}$ = 8.2 Hz, Ir–H), 0.86 [s, 9H, Si(*t*-Bu)], 1.18 [s, 9H, Si(*t*-Bu)], 1.80 (d, 9H, $^2J_{PH}$ = 9.6 Hz, $PMe_3$), 2.59 (d, 1H, $^2J_{HH}$ = 15.0 Hz, $SiCH_2$), 2.81 (d, 1H, $^2J_{HH}$ = 15.0 Hz, $SiCH_2$), 7.49–7.56 (m, 2H, bpy-H$^5$ + bpy-H$^{5'}$), 7.73 (t, 1H, $^3J_{HH}$ = 7.7 Hz, bpy-H$^4$), 7.79 (d, 1H, $^3J_{HH}$ = 7.7 Hz, bpy-H$^3$), 7.94 (td, 1H, $^3J_{HH}$ = 7.8 Hz, $^4J_{HH}$ = 1.5 Hz, bpy-H$^{4'}$), 8.07 (d, 1H, $^3J_{HH}$ = 7.8 Hz, bpy-H$^{3'}$), 8.92 (d, 1H, $^3J_{HH}$ = 5.3 Hz, bpy-H$^{6'}$).[S6] $^{13}$C{$^1$H} NMR (101 MHz, r.t., $CD_2Cl_2$): $\delta$ 21.26 [Si*C*$(CH_3)_3$], 21.34 (d, $^2J_{PC}$ = 38.3 Hz, $PMe_3$), 24.2 [Si*C*$(CH_3)_3$], 29.8 [SiC(*C*$H_3)_3$], 31.6 [SiC(*C*$H_3)_3$], 36.0 ($SiCH_2$), 118.3 (d, $^4J_{PC}$ = 2.1 Hz, bpy-C$^3$), 123.1 (bpy-C$^{3'}$), 124.4 (d, $^4J_{PC}$ = 2.5 Hz, bpy-C$^5$), 125.7 (bpy-C$^{5'}$), 136.7 (bpy-C$^4$), 137.3 (bpy-C$^{4'}$), 150.5 (bpy-C$^{6'}$), 154.9 (bpy-C$^2$), 158.8 (bpy-C$^{2'}$), 170.9 (bpy-C$^6$).[S6] $^{29}$Si{$^1$H} NMR (79.5 MHz, r.t., IG, $CD_2Cl_2$): $\delta$ 16.1 (d, $^2J_{SiP}$ = 13.4 Hz). $^{31}$P{$^1$H} NMR (162 MHz, $CD_2Cl_2$): $\delta$ –47.6. IR (KBr pellet, cm$^{-1}$): 2243 (w, $\nu_{Ir–H}$). HRMS (ESI, positive, additive: NaI): *m*/*z* calcd for [$^{12}C_{22}{}^1H_{37}{}^{14}N_2{}^{28}Si{}^{31}P{}^{35}Cl{}^{193}Ir$ + $^{23}Na$]$^+$ ([M + Na]$^+$) 639.1674, found 639.1674. Anal. Calcd for $C_{22}H_{37}N_2SiPClIr$: C, 42.88; H, 6.05; N, 4.55. Found: C, 42.99; H, 6.11; N, 4.56.

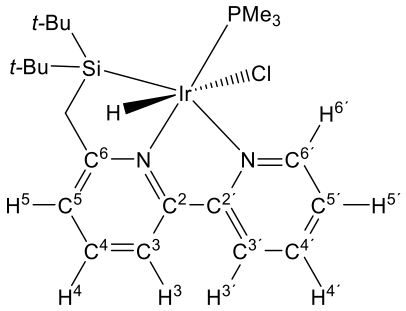

### 1.6 Catalytic C–H borylation of arenes

***1.6.1 General procedure for NMR monitoring of reactions of benzene with $B_2pin_2$ or HBpin in the presence of a catalytic amount of 1, A, 2 or 3.*** An NMR tube equipped with a Teflon needle valve was charged with bis(pinacolato)diboron $B_2pin_2$ (51 mg, 0.20 mmol) or pinacolborane HBpin (57.5 μL, $d$ = 0.89 g $mL^{-1}$, 0.40 mmol), $Si(SiMe_3)_4$ or $C_6Me_6$ (< 1 mg, internal standard) and a sealed glass capillary containing $C_6D_6$ (an external lock solvent). $B_2pin_2$/HBpin and the internal standard were dissolved in $C_6H_6$ (0.89 mL, $d$ = 0.88 g $mL^{-1}$, 10 mmol), and the solution was placed into the NMR tube. A $^1H$ NMR spectrum of the solution was recorded, and the intensity ratio of the $^1H$ signals between $B_2pin_2$ or HBpin and the internal standard was determined. A catalytic amount of complex **1**, **A**, **2** or **3** (2 μmol; 1 or 0.5 mol% based on $B_2pin_2$ or HBpin, respectively) was then added to the solution. In the case of the reaction using catalyst **3**, THF (0.2 mL) was added to the reaction mixture to increase the amount of dissolution of **3**. The mixture was heated at 40 °C in most cases. In some cases, the mixture was allowed to stand at room temperature (ca. 20 °C) or heated at 80 °C. The reaction was monitored employing $^1H$ and $^{11}B$ NMR spectroscopy. NMR yield of the C–H borylation product PhBpin was determined by comparison of the intensity of the $^1H$ NMR signals of PhBpin with that for the internal standard. A plot of a time course of the boron-containing species $B_2pin_2$, HBpin and $C_6H_5Bpin$ in the reaction mixture of the C–H borylation of benzene catalysed by **1** at 40 °C is depicted in Fig. S1 (page S15). PhBpin was identified by comparison of $^1H$ and $^{13}C\{^1H\}$ NMR spectroscopic data with the literature data.[S7]

***1.6.2 NMR monitoring of C–D borylation of benzene-$d_6$ catalysed by 1.*** This borylation was monitored by a procedure similar to that for the general procedure described in 1.6.1 by use of a solution of $B_2pin_2$ (51 mg, 0.20 mmol), $Si(SiMe_3)_4$ (< 1 mg, internal standard) and complex **1** (1 mg, 2 μmol; 1 mol%) in $C_6D_6$ (0.89 mL, $d$ = 0.95 g·$mL^{-1}$, 10 mmol).

After heating of the solution for 50 h at 40 °C, the borylation product $(C_6D_5)$Bpin was formed in 97% NMR yield.

***1.6.3 Procedure for C–H borylation of monosubstituted arenes catalysed by 1: NMR monitoring and isolation of an isomeric mixture of arylboronate esters.*** A procedure similar to the NMR monitoring of the catalytic C–H borylation of benzene described in section 1.6.1 was applied by use of complex **1** (1 mg, 2 μmol; 1 mol%), arene (toluene, bromobenzene or fluorobenzene) (5 mmol), $B_2pin_2$ (51 mg, 0.20 mmol) and $Si(SiMe_3)_4$ (< 1 mg, internal standard) under neat conditions at 40 ºC. After completion of the reaction, the NMR yield of the total of the arylboronate esters based on boron was calculated by comparing the intensity of the $^1$H NMR signal for the products relative to that of $Si(SiMe_3)_4$ with the corresponding intensity for $B_2pin_2$ before the reaction. The resulting reaction mixture was passed through a short column of silica gel [eluent: hexane/EtOAc (3 : 1)] to remove iridium containing species. Volatiles were removed from the eluate by evaporation under vacuum to give an isomeric mixture of the C–H borylation products (arylboronate esters) as a colourless oil in 93–99% isolated yield. The products were identified by comparison of $^1$H and $^{13}$C{$^1$H} NMR spectroscopic data with the literature data.[S7,S8] Assignment of the $^1$H and $^{13}$C NMR signals of each regioisomer in the isomeric mixture was confirmed based on the $^1$H–$^{13}$C HSQC and HMBC spectra. The ratio of regioisomers was determined by $^1$H NMR spectroscopy. NMR data for the arylboronate esters are indicated below.

**NMR spectroscopic data for arylboronate esters**

***PhBpin (phenylboronic acid pinacol ester)***

$^{1}$H NMR [400 MHz, r.t., $C_6H_6$ ($C_6D_6$ in a capillary for external lock)]: $\delta$ 1.11 (s, 12H, Bpin), 7.20–7.24 (m, 3H, Ar-H), 8.10–8.15 (m, 2H, Ar-H). The $^{1}$H NMR chemical shifts were referenced to $C_6H_6$ (7.15 ppm).

$^{11}$B{$^{1}$H} NMR [128 MHz, r.t., $C_6H_6$ ($C_6D_6$ in a capillary for external lock)]: $\delta$ 31.1.

$^{13}$C{$^{1}$H} NMR [101 MHz, r.t., $C_6H_6$ ($C_6D_6$ in a capillary for external lock)]: $\delta$ 24.9 [Bpin(OC*Me*$_2$)], 83.7 [Bpin(O*C*Me$_2$)], 128.0 (Ar-C), 131.5 (Ar-C), 135.4 (Ar-C).[S9]

***($C_6D_5$)Bpin [(2,3,4,5,6-pentadeuteriophenyl)boronic acid pinacol ester]***

$^{1}$H NMR (400 MHz, r.t., $C_6D_6$): $\delta$ 1.11 (s, 12H, Bpin).

$^{11}$B{$^{1}$H} NMR (128 MHz, r.t., $C_6D_6$): $\delta$ 31.1.

***m-($C_6H_4$Me)Bpin [(3-methylphenyl)boronic acid pinacol ester]***

$^{1}$H NMR (400 MHz, r.t., $CDCl_3$): $\delta$ 1.36 (s, 12H, Bpin), 2.37 (s, 3H, $C_6H_4$*Me*), 7.26–7.31 (m, 2H, Ar-H), 7.61–7.66 (m, 1H, Ar-H), 7.66 (br s, 1H, Ar-H).

$^{11}$B{$^{1}$H} NMR (128 MHz, r.t., $CDCl_3$): $\delta$ 30.9.

$^{13}$C{$^{1}$H} NMR (101 MHz, r.t., $CDCl_3$): $\delta$ 21.2 ($C_6H_4$*Me*), 24.8 [Bpin(OC*Me*)], 83.6 [Bpin(O*C*Me)], 127.6 (Ar-C), 131.8 (Ar-C), 132.0 (Ar-C), 135.3 (Ar-C), 137.0 (Ar-C).[S9]

***p-($C_6H_4$Me)Bpin [(4-methylphenyl)boronic acid pinacol ester]***

$^{1}$H NMR (400 MHz, r.t., $CDCl_3$): $\delta$ 1.35 (s, 12H, Bpin), 2.38 (s, 3H, $C_6H_4$*Me*), 7.20 (br d, 2H, $^{3}J_{HH}$ = 7.8 Hz, Ar-H), 7.73 (br d, 2H, $^{3}J_{HH}$ = 7.8 Hz, Ar-H).

$^{11}$B{$^{1}$H} NMR (128 MHz, r.t., $CDCl_3$): $\delta$ 30.9.

$^{13}$C{$^{1}$H} NMR (101 MHz, r.t., $CDCl_3$): $\delta$ 21.7 ($C_6H_4$*Me*), 24.8 [Bpin(OC*Me*$_2$)], 83.5 [Bpin(O*C*Me$_2$)], 128.5 (Ar-C), 134.8 (Ar-C), 141.3 (Ar-C).[S9]

***m*-($C_6H_4Br$)Bpin [(3-bromophenyl)boronic acid pinacol ester]**

$^1$H NMR (400 MHz, r.t., $CDCl_3$): $\delta$ 1.35 (s, 12H, Bpin), 7.24 (t, 1H, $^3J_{HH}$ = 7.7 Hz, Ar-H), 7.58 (br d, 1H, $^3J_{HH}$ = 7.7 Hz, Ar-H), 7.73 (d, 1H, $^3J_{HH}$ = 7.7 Hz, Ar-H), 7.96 (br s, 1H, Ar-H).

$^{11}$B{$^1$H} NMR (128 MHz, r.t., $CDCl_3$): $\delta$ 30.4.

$^{13}$C{$^1$H} NMR (101 MHz, r.t., $CDCl_3$): $\delta$ 24.8 [Bpin(OC*Me*$_2$)], 84.1 [Bpin(O*C*Me$_2$)], 122.4 (Ar-C), 129.4 (Ar-C), 133.1 (Ar-C), 134.1 (Ar-C), 137.4 (Ar-C).[S9]

***p*-($C_6H_4Br$)Bpin [(4-bromophenyl)boronic acid pinacol ester]**

$^1$H NMR (400 MHz, r.t., $CDCl_3$): $\delta$ 1.34 (s, 12H, Bpin), 7.51 (d, 2H, $^3J_{HH}$ = 8.1 Hz, Ar-H), 7.68 (d, 2H, $^3J_{HH}$ = 8.1 Hz, Ar-H).

$^{11}$B{$^1$H} NMR (128 MHz, r.t., $CDCl_3$): $\delta$ 30.4.

$^{13}$C{$^1$H} NMR (101 MHz, r.t., $CDCl_3$): $\delta$ 24.8 [Bpin(OC*Me*$_2$)], 83.9 [Bpin(O*C*Me$_2$)], 126.2 (Ar-C), 136.3 (Ar-C).[S9]

***o*-($C_6H_4F$)Bpin [(2-fluorophenyl)boronic acid pinacol ester]**

$^1$H NMR (400 MHz, r.t., $CDCl_3$): $\delta$ 1.35 (s, 12H, Bpin), 6.98–7.04 (m, 1H, Ar-H), 7.09–7.15 (m, 1H, Ar-H), 7.41 (dddd, 1H, *J* = 8.2, 7.4, 5.6, 1.9 Hz, Ar-H), 7.74 (ddd, 1H, *J* = 7.4, 6.2, 1.9 Hz, Ar-H).

$^{11}$B{$^1$H} NMR (128 MHz, r.t., $CDCl_3$): $\delta$ 30.3.

$^{13}$C{$^1$H} NMR (101 MHz, r.t., $CDCl_3$): $\delta$ 24.8 [Bpin(OC*Me*$_2$)], 83.8 [Bpin(O*C*Me$_2$)], 115.2 (d, $J_{CF}$ = 24 Hz, Ar-C), 123.5 (d, $J_{CF}$ = 3 Hz, Ar-C), 133.2 (d, $J_{CF}$ = 9 Hz, Ar-C), 136.8 (d, $J_{CF}$ = 7 Hz, Ar-C), 167.2 [d, $^1J_{CF}$ = 250 Hz, Ar-C(C–F)].[S9]

$^{19}$F{$^1$H} NMR (376 MHz, r.t., $CDCl_3$): $\delta$ –102.5.

***m*-($C_6H_4F$)Bpin [(3-fluorophenyl)boronic acid pinacol ester]**

$^1$H NMR (400 MHz, r.t., $CDCl_3$): $\delta$ 1.33 (s, 12H, Bpin), 7.09–7.15 (m, 1H, Ar-H), 7.32 (ddd, 1H, *J* = 8.2, 7.4, 5.5 Hz, Ar-H), 7.48 (br dd, 1H, *J* = 9.2, 2.7 Hz, Ar-H), 7.57 (br dd, 1H, *J* = 7.4, 0.6 Hz, Ar-H).

$^{11}$B{$^1$H} NMR (128 MHz, r.t., $CDCl_3$): $\delta$ 30.3.

$^{13}$C{$^1$H} NMR (101 MHz, r.t., $CDCl_3$): $\delta$ 24.8 [Bpin(OC*Me*$_2$)], 84.0 [Bpin(O*C*Me$_2$)], 118.1 (d, $J_{CF}$ = 21 Hz, Ar-C), 120.9 (d, $J_{CF}$ = 20 Hz, Ar-C), 129.4 (d, $J_{CF}$ = 7 Hz, Ar-C), 130.3 (d, $J_{CF}$ = 3 Hz, Ar-C), 162.5 [d, $^1J_{CF}$ = 246 Hz, Ar-C(C–F)].[S9]

$^{19}$F{$^1$H} NMR (376 MHz, r.t., $CDCl_3$): $\delta$ –114.2.

***p*-($C_6H_4F$)Bpin [(4-fluorophenyl)boronic acid pinacol ester]**

$^1$H NMR (400 MHz, r.t., $CDCl_3$): $\delta$ 1.32 (s, 12H, Bpin), 7.00–7.07 (m, 2H, Ar-H), 7.76–7.83 (m, 2H, Ar-H).

$^{11}$B{$^1$H} NMR (128 MHz, r.t., $CDCl_3$): $\delta$ 30.3.

$^{13}$C{$^1$H} NMR (101 MHz, r.t., $CDCl_3$): $\delta$ 24.8 [Bpin(OC*Me*$_2$)], 83.8 [Bpin(O*C*Me$_2$)], 114.8 (d, $J_{CF}$ = 20 Hz, Ar-C), 137.0 (d, $J_{CF}$ = 9 Hz, Ar-C), 165.1 [d, $^1J_{CF}$ = 251 Hz, Ar-C(C–F)].[S9]

$^{19}$F{$^1$H} NMR (376 MHz, r.t., $CDCl_3$): $\delta$ –108.4.

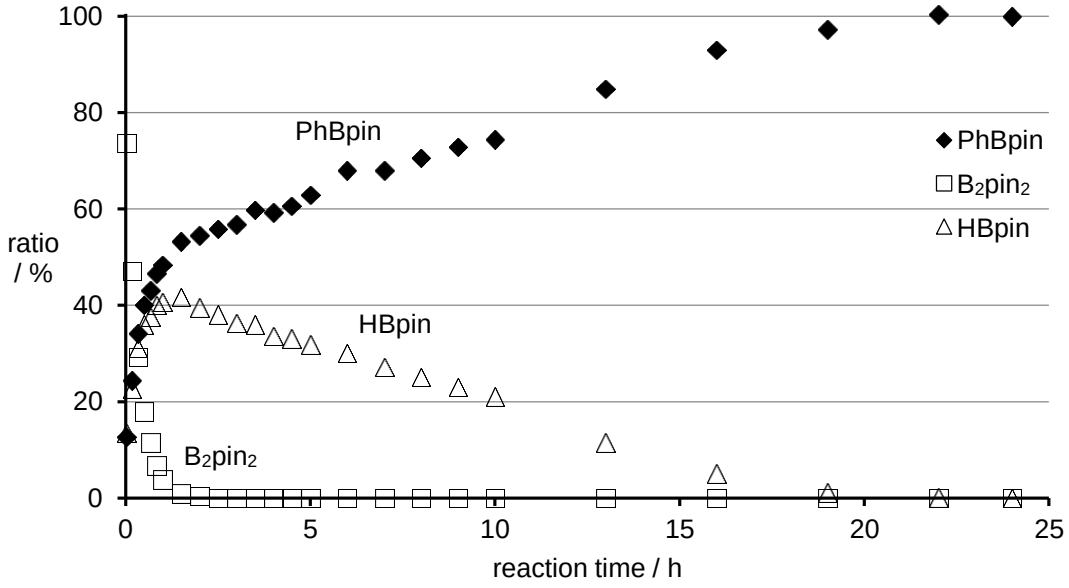


**Fig. S1** Time course of the boron-containing species in a reaction mixture of the C−H borylation of benzene with $B_2pin_2$ catalysed by complex **1** at 40 °C. Ratios (%) of these species are determined by $^1H$ NMR based on the molar amount of $B_2pin_2$ before reaction.

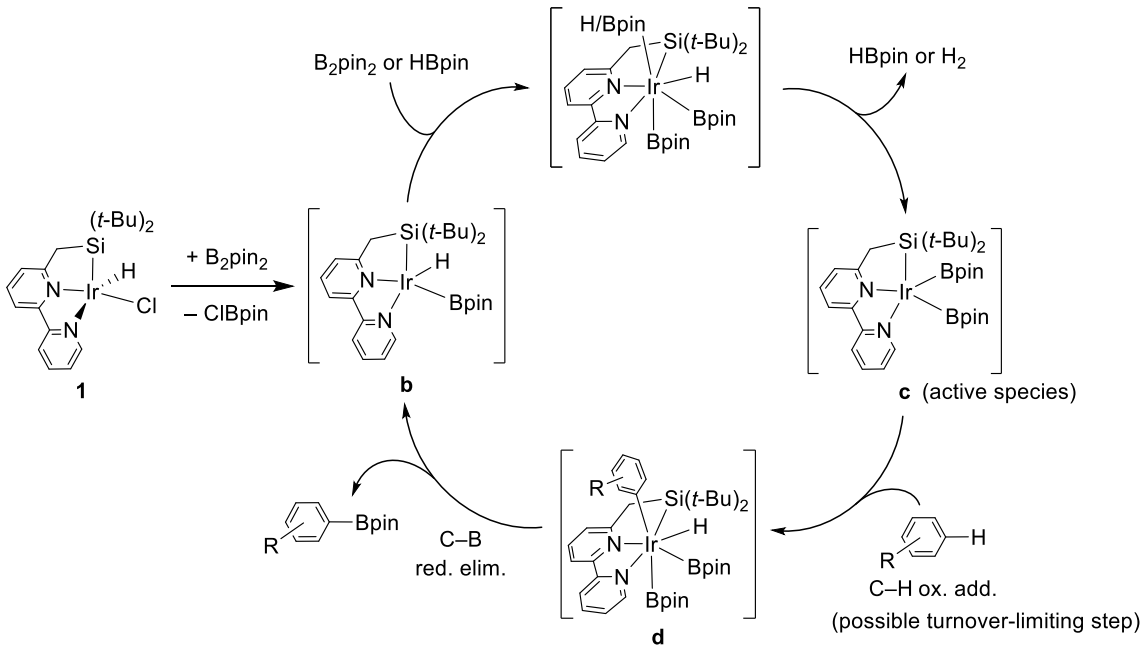


**Scheme S1** Proposed mechanism for the arene C–H borylation catalysed by **1**.

## 2. X-ray crystal structure analysis of complexes 1–3

X-ray-quality single crystals of **1** and **3** were obtained by slow diffusion of hexane into a solution in THF (for **1**) or $CH_2Cl_2$ (for **3**) at room temperature as black block crystals and orange block crystals, respectively. Single crystals of **2** were obtained by crystallization directly from a reaction mixture of $[RhCl(coe)]_2$ and $Bpy^{SiNN}(H)$ in benzene-$d_6$ as dark-red plate crystals. The intensity data for the analysis were collected on a Rigaku RAXIS-RAPID imaging plate diffractometer with graphite monochromated Mo Kα radiation ($\lambda$ = 0.71073 Å) under a cold nitrogen stream ($T$ = 150 K). A numerical absorption correction was applied to the data. The structures were solved according to the Patterson method using the DIRDIF-2008 program[S10] refined by full-matrix least-squares techniques on all $F^2$ data with SHELXL-2018/1.[S11] Anisotropic refinement was applied to all non-hydrogen atoms. The hydrido hydrogen of each of complexes **1–3** was located on the difference Fourier map and refined isotropically. The Ir–H(hydrido) distance for **1** was restrained to 1.60(1) Å using DFIX instruction in SHELXL.[S12] The other hydrogen atoms were placed at the calculated positions. Some reflections, that is, (*h k l*) = (1 0 0), (0 0 2) and (0 1 1) for **1**; (*h k l*) = (1 0 0), (0 1 1) and (1 1 0) for **2**, (*h k l*) = (0 0 1) and (1 1 0) for **3** were omitted from the final refinement because their intensities were significantly weakened by the beam stop. All calculations were performed using the Yadokari-XG.[S13] Crystallographic data and selected bond distances and angles for **1–3** are listed in Tables S1 and S2, respectively. Molecular structure of **2** is depicted in Fig. S2. CCDC reference numbers: 2167507 (for **1**), 2167508 (for **2**) and 2167509 (for **3**). The crystallographic data are available as a CIF file.

**Table S1** Crystallographic data for M(Bpy$^{SiNN}$)(H)Cl [M = Ir (**1**) and Rh (**2**)] and Ir(Bpy$^{SiNN}$)(H)(PMe$_3$)Cl (**3**)

| Compound | **1** | **2** | **3** |
|---|---|---|---|
| formula | $C_{19}H_{28}N_2SiClIr$ | $C_{19}H_{28}N_2SiClRh$ | $C_{22}H_{37}N_2SiPClIr$ |
| formula weight | 540.17 | 450.88 | 616.24 |
| crystal system | monoclinic | monoclinic | monoclinic |
| crystal size/mm$^3$ | 0.20 × 0.15 × 0.15 | 0.18 × 0.14 × 0.06 | 0.25 × 0.23 × 0.22 |
| space group | $P2_1/c$ (No. 14) | $P2_1/c$ (No. 14) | $P2_1/a$ (No. 14) |
| $a$/Å | 13.0266(10) | 15.0274(15) | 15.8176(8) |
| $b$/Å | 9.0938(5) | 14.7588(13) | 9.3483(4) |
| $c$/Å | 17.1609(7) | 9.1280(11) | 18.1721(9) |
| $\alpha$/° | 90 | 90 | 90 |
| $\beta$/° | 96.959(4) | 95.520(4) | 110.406(2) |
| $\gamma$/° | 90 | 90 | 90 |
| $V$/Å$^3$ | 2017.9(2) | 2015.1(4) | 2518.4(2) |
| $Z$ | 4 | 4 | 4 |
| $D_{calcd}$/g·cm$^{-3}$ | 1.778 | 1.486 | 1.625 |
| $F$(000) | 1056 | 928 | 1224 |
| $\mu$(Mo-K$\alpha$)/mm$^{-1}$ | 6.812 | 1.043 | 5.529 |
| reflections collected | 20365 | 19098 | 28834 |
| unique reflections ($R_{int}$) | 4608 (0.1109) | 4613 (0.0475) | 5774 (0.1009) |
| refined parameters | 227 | 227 | 266 |
| $R1$, $wR2$ (all data)[a,b] | 0.0393, 0.0977 | 0.0376, 0.0641 | 0.0314, 0.0759 |
| $R1$, $wR2$ [$I > 2\ \sigma(I)$][a,b] | 0.0360, 0.0948 | 0.0320, 0.0625 | 0.0298, 0.0747 |
| GOF | 1.153 | 1.172 | 1.112 |
| largest residual peak, hole/e·Å$^{-3}$ | 3.171, –1.194 | 0.400, –0.381 | 2.065, –1.312 |

[a] $R1 = \Sigma\ ||F_o| - |F_c|| / \Sigma\ |F_o|$, [b] $wR2 = \{\Sigma\ [w\ (F_o^2 - F_c^2)^2] / \Sigma\ [w\ (F_o^2)^2]\}^{1/2}$

**Table S2** Selected bond distances (Å) and angles (°) for **1–3**

| compound | **1** | **2** | **3** |
|---|---|---|---|
| Ir/Rh–Si | 2.2771(14) | 2.2955(7) | 2.3588(9) |
| Ir/Rh–N1 | 1.990(3) | 2.0118(18) | 2.100(3) |
| Ir/Rh–N2 | 2.115(4) | 2.1133(19) | 2.217(2) |
| Ir/Rh–Cl | 2.3334(10) | 2.3298(6) | 2.5079(8) |
| Ir–P | | | 2.2378(8) |
| Ir/Rh–H1 | ca. 1.6 | 1.49(3) | 1.63(4) |
| Si···H1 | ca. 2.5 | 1.89(3) | 2.58(5) |
| | | | |
| Si–Ir/Rh–N1 | 81.84(12) | 82.28(6) | 83.19(8) |
| Si–Ir/Rh–N2 | 132.52(10) | 143.56(5) | 157.65(7) |
| N1–Ir/Rh–N2 | 78.67(14) | 79.21(7) | 75.73(10) |
| Si–Ir/Rh–Cl | 106.88(4) | 102.21(2) | 98.83(3) |
| Cl–Ir/Rh–N1 | 171.22(12) | 175.07(6) | 87.69(7) |
| Cl–Ir/Rh–N2 | 95.65(10) | 95.90(5) | 87.77(7) |
| Si–Ir–P | | | 101.93(3) |
| Cl–Ir–P | | | 97.27(3) |
| Si–Ir/Rh–H1 | ca. 80 | 55.1(12) | 78.3(16) |
| N1–Ir/Rh–H1 | ca. 100 | 97.9(12) | 91.3(14) |
| N2–Ir/Rh–H1 | ca. 150 | 158.7(12) | 94.7(16) |
| Cl–Ir/Rh–H1 | ca. 80 | 86.5(12) | 177.1(16) |
| P–Ir–H1 | | | 84.0(14) |
| Ir/Rh–H1–Si | ca. 60 | 84.6(14) | 63.6(16) |

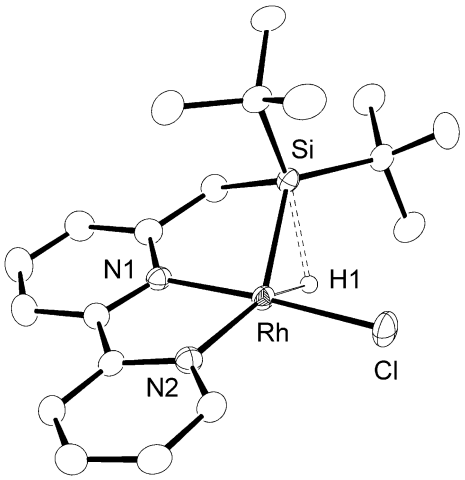


**Fig. S2** Molecular structure of Rh(Bpy$^{SiNN}$)(H)Cl (**2**). The Si···H distance [1.89(3) Å] is relatively short, implying the existence of weak interaction between the silyl and hydrido ligands (1.9–2.1 Å[S14] for Si···H interaction). This interaction is also suggested in solution by the relatively large satellite Si–H coupling ($J_{SiH}$ = 39 Hz > 20 Hz[S15]) observed for Rh–H in the $^1$H NMR spectrum.

## 3. References


S1 J. Peng and Y. Kishi, *Org. Lett.*, 2012, **14**, 86–89.

S2 M. Weidenbruch, A. Schäfer and A. Lesch, in *Synthetic Methods of Organometallic and Inorganic Chemistry*, ed. W. A. Herrmann (vol. eds. N. Auner and U. Klingebiel), Georg Thieme Verlag, Stuttgart, New York, 1996, vol. 2, pp. 210–213.

S3 J. L. Herde, J. C. Lambert and C. V. Senoff, *Inorg. Synth.*, 1974, **15**, 18–20.

S4 A. van der Ent, A. L. Onderdelinden and R. A. Schunn, *Inorg. Synth.*, 1973, **14**, 92–95.

S5 T. Komuro, T. Osawa, R. Suzuki, D. Mochizuki, H. Higashi and H. Tobita, *Chem. Commun.*, 2019, **55**, 957–960.

S6 $^{1}$H and $^{13}$C{$^{1}$H} NMR signals of Bpy$^{SiNN}$(H) and complexes **1–3** were assigned based on $^{1}$H–$^{13}$C HSQC and $^{1}$H–$^{13}$C HMBC spectra.

S7 (a) M. Tobisu, T. Igarashi and N. Chatani, *Beilstein J. Org. Chem.*, 2016, **12**, 654–661; (b) A. M. Mfuh, J. D. Doyle, B. Chhetri, H. D. Arman and O. V. Larionov, *J. Am. Chem. Soc.*, 2016, **138**, 2985–2988.

S8 (a) M. A. Esteruelas, A. Martínez, M. Oliván and E. Oñate, *Chem. Eur. J.*, 2020, **26**, 12632–12644; (b) M. A. Esteruelas, M. Oliván and A. Vélez, *Organometallics*, 2015, **34**, 1911–1924; (c) F. Labre, Y. Gimbert, P. Bannwarth, S. Olivero, E. Duñach and P. Y. Chavant, *Org. Lett.*, 2014, **16**, 2366–2369; (d) J. Zhou, M. W. Kuntze-Fechner, R. Bertermann, U. S. D. Paul, J. H. J. Berthel, A. Friedrich, Z. Du, T. B. Marder and U. Radius, *J. Am. Chem. Soc.*, 2016, **138**, 5250–5253.

S9 The $^{13}$C NMR signal of the boron-substituted carbon of arylboronate ester was not observed.

S10 P. T. Beurskens, G. Beurskens, R. de Gelder, S. Garcia-Granda, R. O. Gould and J. M. M. Smits, *The DIRDIF2008 program system*, Crystallography Laboratory, University of Nijmegen, The Netherlands, 2008.

S11 (a) G. M. Sheldrick, *Acta Crystallogr., Sect. C: Struct. Chem.*, 2015, **71**, 3–8; (b) G. M. Sheldrick, *Acta Crystallogr., Sect. A: Found. Adv.*, 2008, **64**, 112–122.

S12 E. M. Pelczar, T. J. Emge and A. S. Goldman, *Acta Crystallogr., Sect. C: Cryst. Struct. Commun.*, 2007, **63**, m323–m326.

S13 (a) K. Wakita, *Yadokari-XG, Software for Crystal Structure Analyses*, 2001. (b) C. Kabuto, S. Akine, T. Nemoto and E. Kwon, Release of Software (Yadokari-XG 2009) for Crystal Structure Analyses, *J. Crystallogr. Soc. Jpn.*, 2009, **51**, 218–224.

S14 Z. Lin, *Chem. Soc. Rev.*, 2002, **31**, 239–245.

S15 (a) J. Y. Corey and J. Braddock-Wilking, *Chem. Rev.*, 1999, **99**, 175–292; (b) J. Y. Corey, *Chem. Rev.*, 2011, **111**, 863–1071.

## 4. NMR spectra of Bpy$^{SiNN}$(H) and complexes 1–3

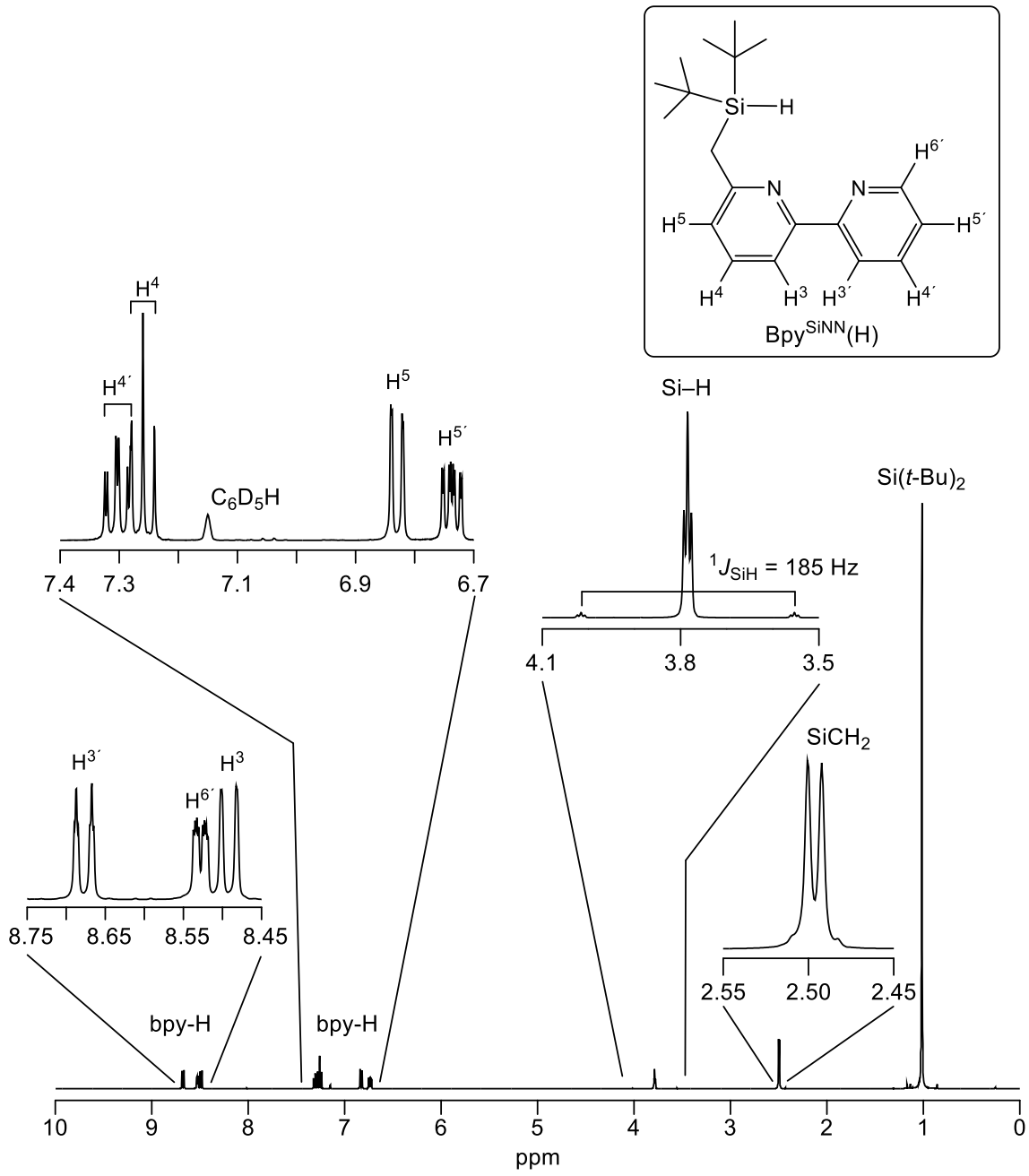


**Fig. S3** $^{1}$H NMR spectrum of 6-di-*tert*-butylsilylmethyl-2,2´-bipyridine [Bpy$^{SiNN}$(H)] (400 MHz, r.t., $C_6D_6$).

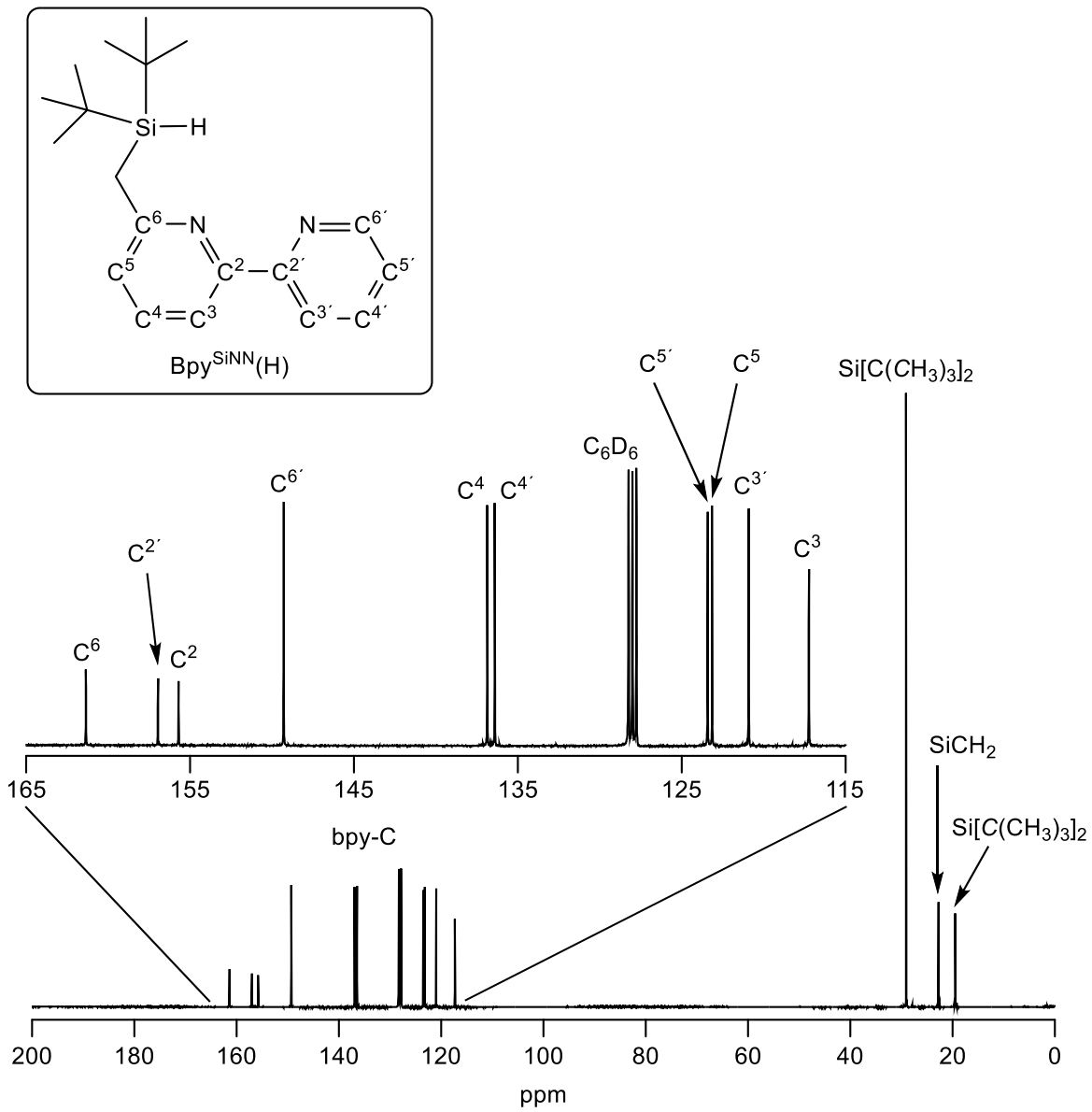


**Fig. S4** $^{13}C\{^{1}H\}$ NMR spectrum of $Bpy^{SiNN}(H)$ (101 MHz, r.t., $C_6D_6$).

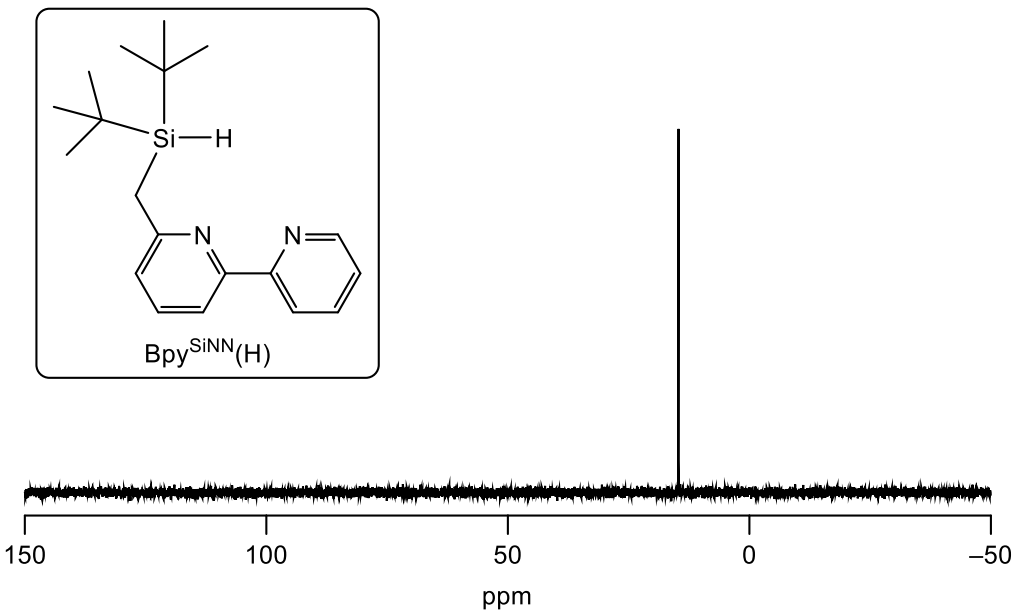


**Fig. S5** $^{29}Si\{^{1}H\}$ NMR spectrum of $Bpy^{SiNN}(H)$ (79.5 MHz, DEPT, r.t., $C_6D_6$).

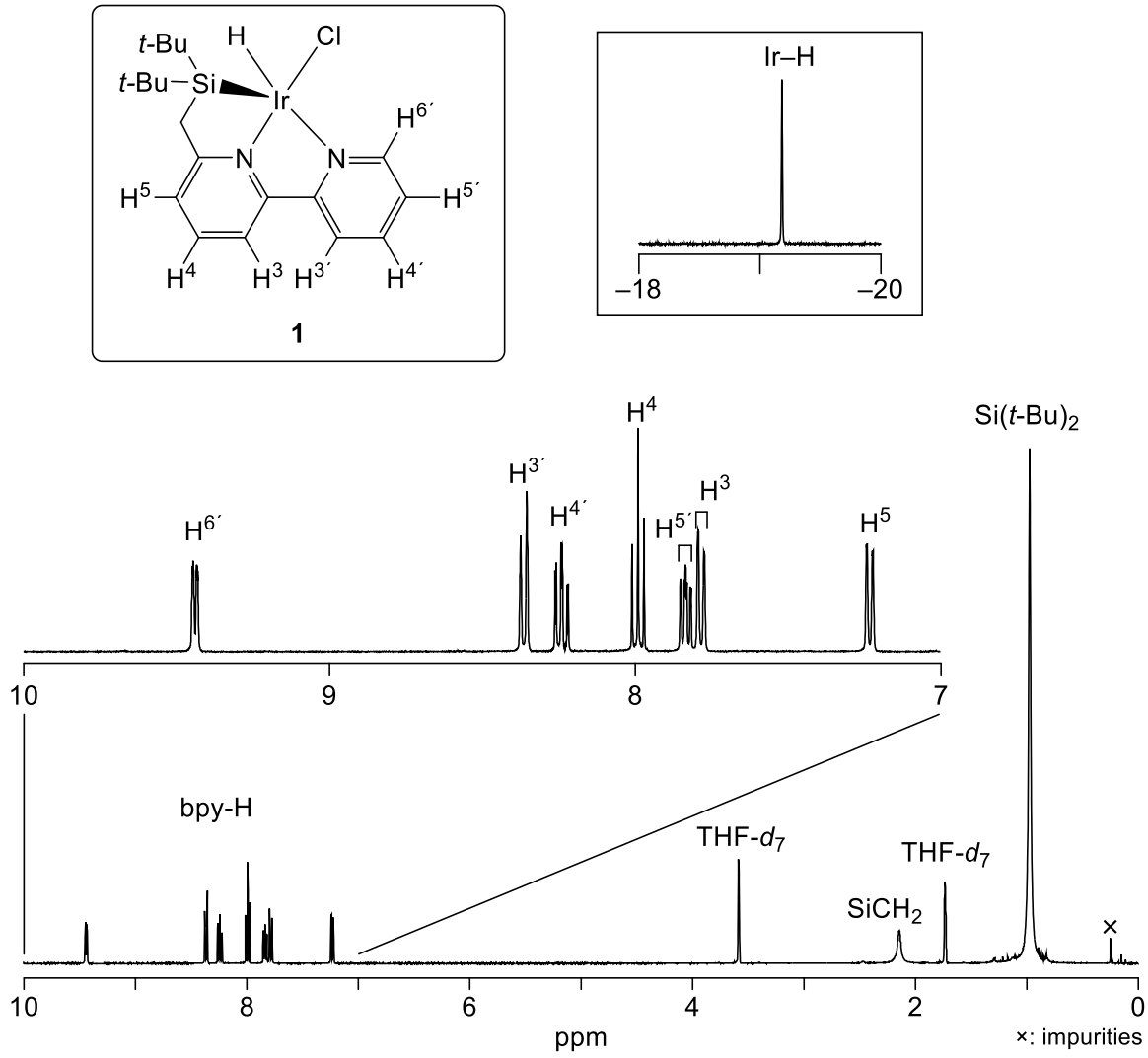


**Fig. S6** $^{1}$H NMR spectrum of Ir(Bpy$^{SiNN}$)(H)Cl (**1**) (400 MHz, r.t., THF-$d_8$).

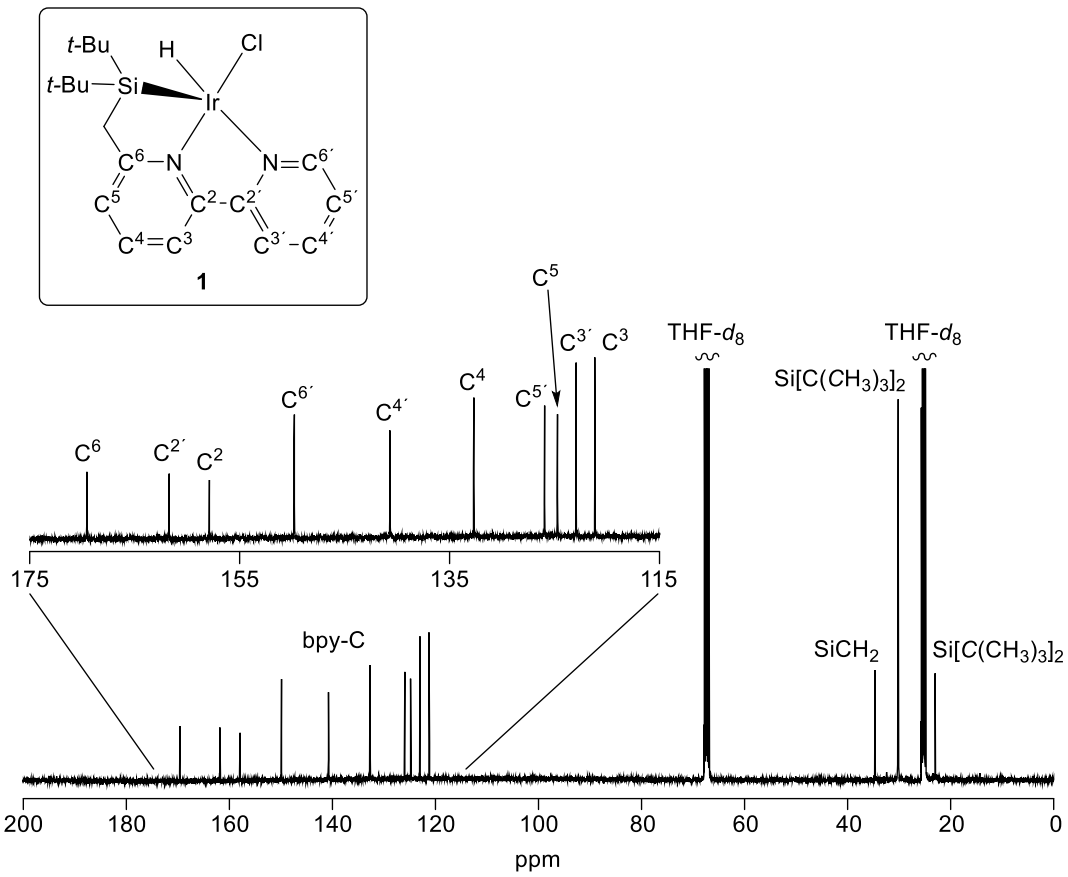


**Fig. S7** $^{13}C\{^{1}H\}$ NMR spectrum of **1** (101 MHz, r.t., THF-$d_8$).

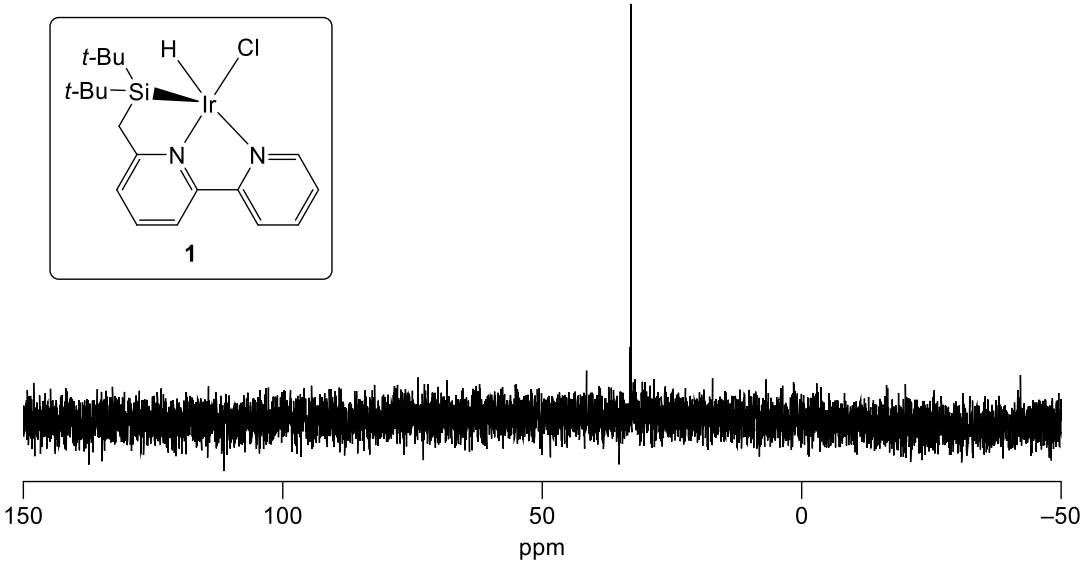


**Fig. S8** $^{29}Si\{^{1}H\}$ NMR spectrum of **1** (79.5 MHz, IG, r.t., THF-$d_8$).

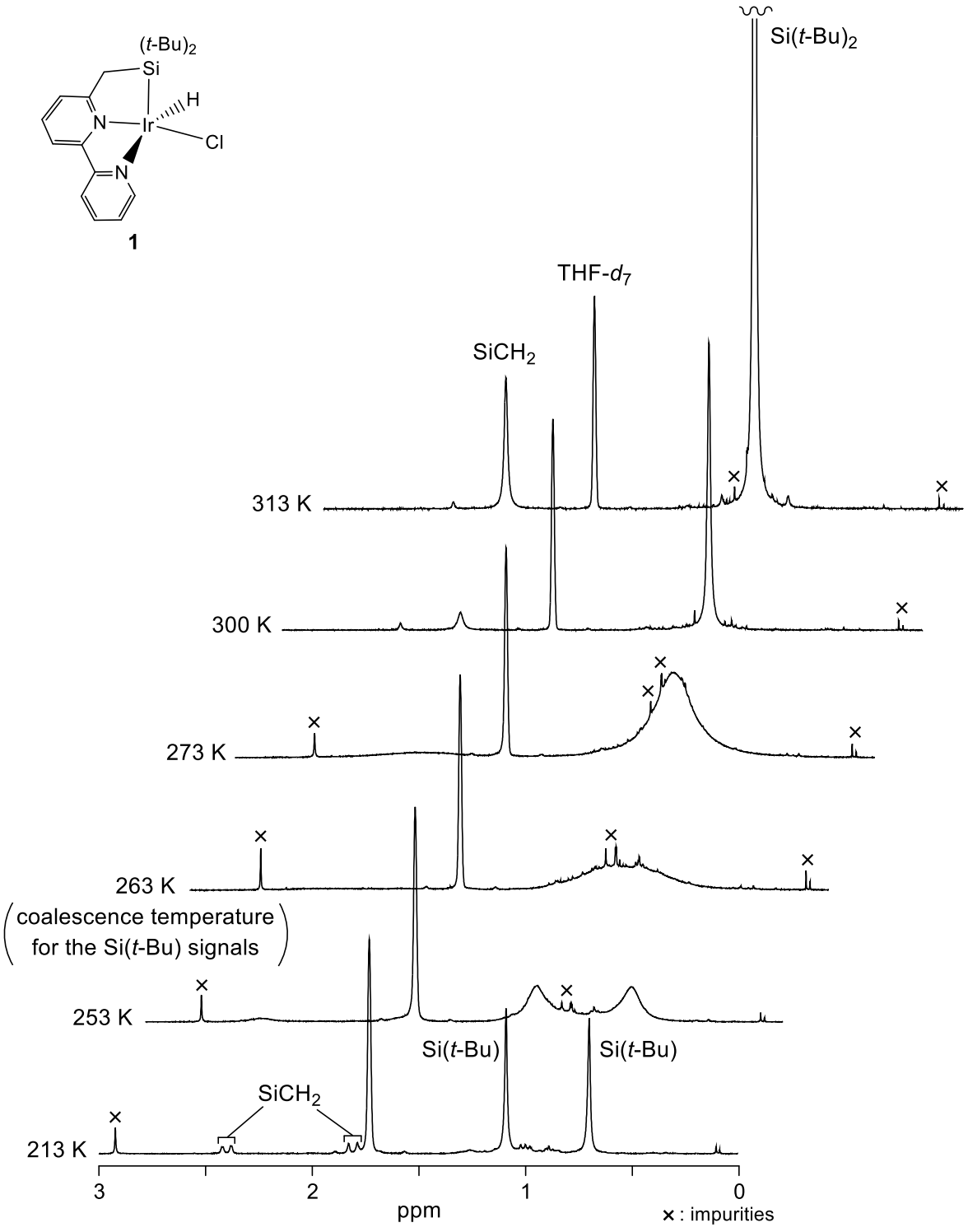


**Fig. S9** Variable-temperature $^{1}$H NMR spectra of Ir(Bpy$^{SiNN}$)(H)Cl (**1**) in the range from 3 to 0 ppm (400 MHz, 313–213 K, THF-$d_8$).

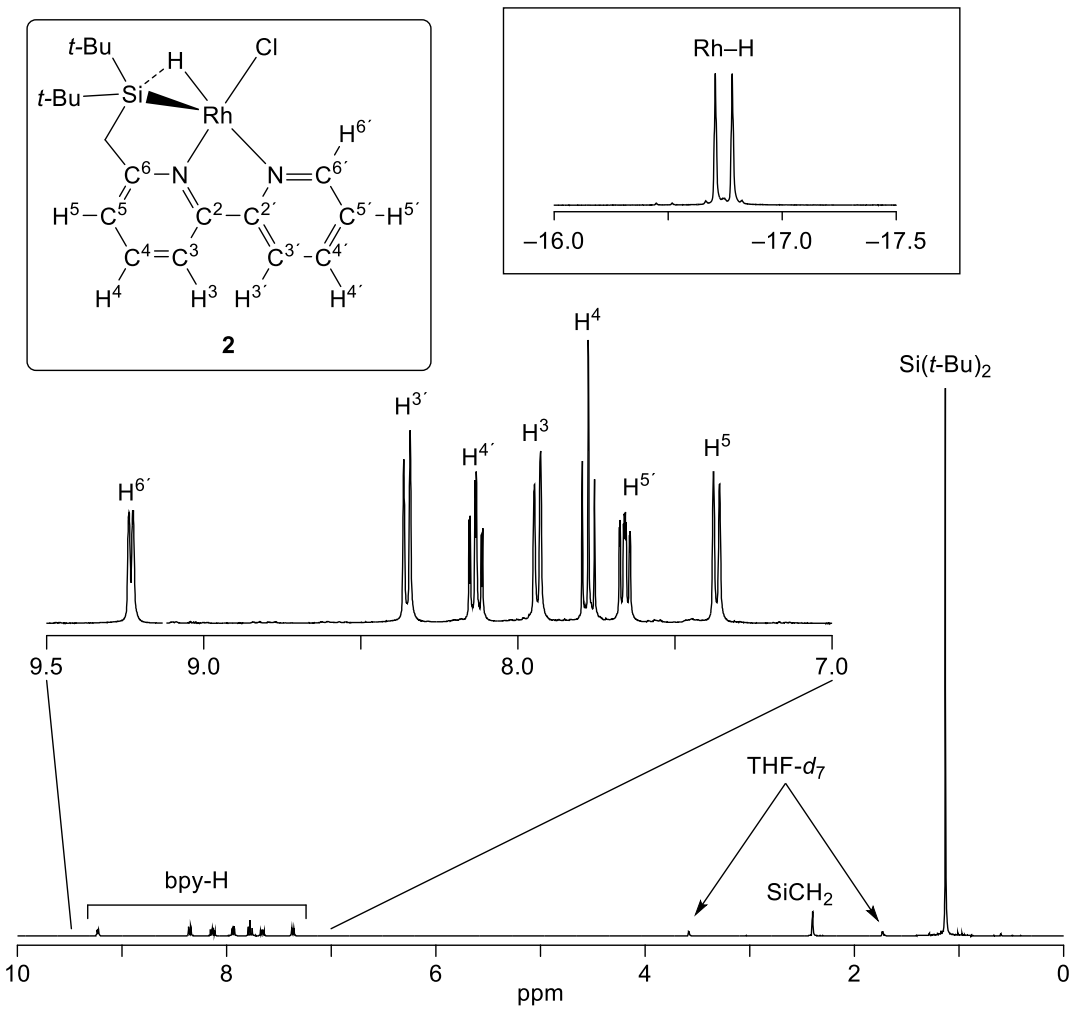


**Fig. S10** $^{1}$H NMR spectrum of Rh(Bpy$^{SiNN}$)(H)Cl (**2**) (400 MHz, r.t., THF-$d_8$).

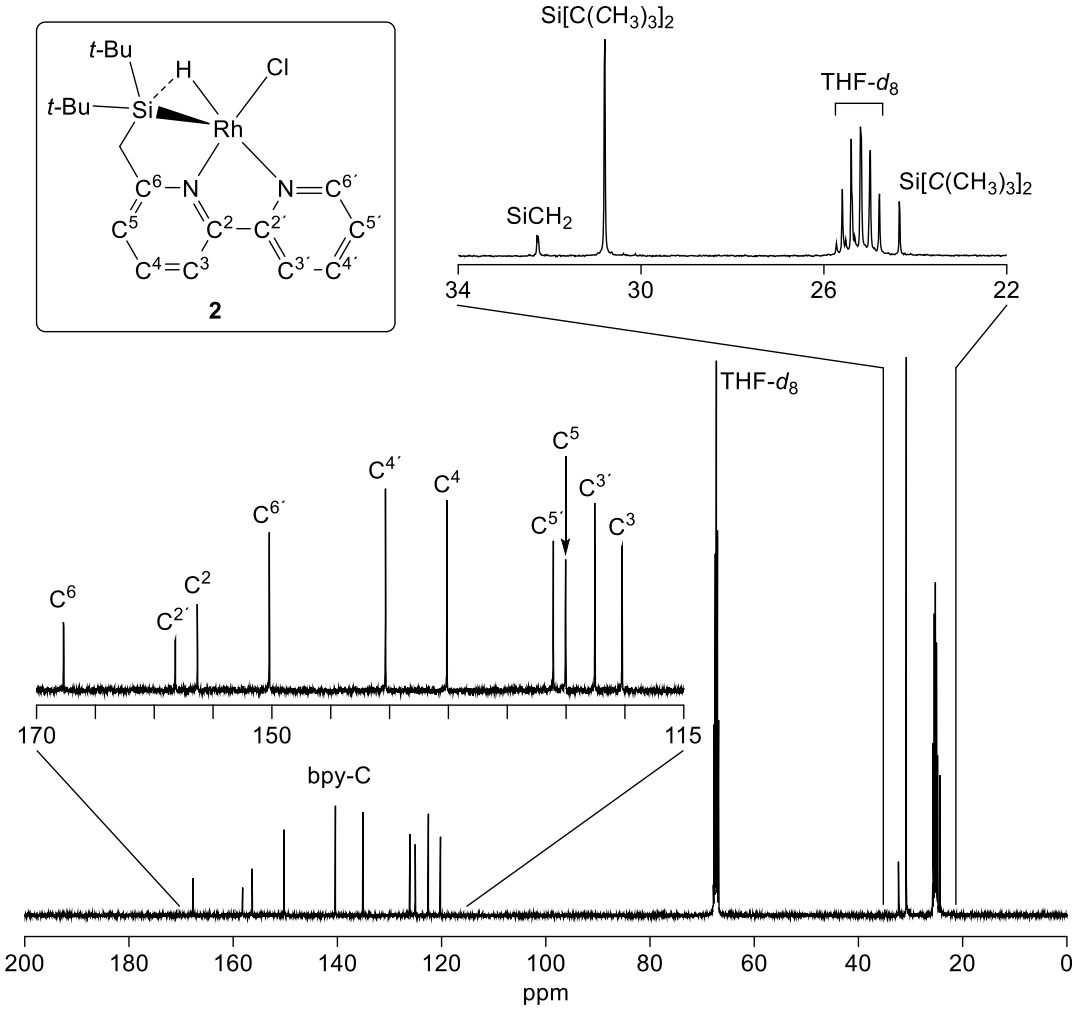


**Fig. S11** $^{13}C\{^{1}H\}$ NMR spectrum of **2** (101 MHz, r.t., THF-$d_8$).

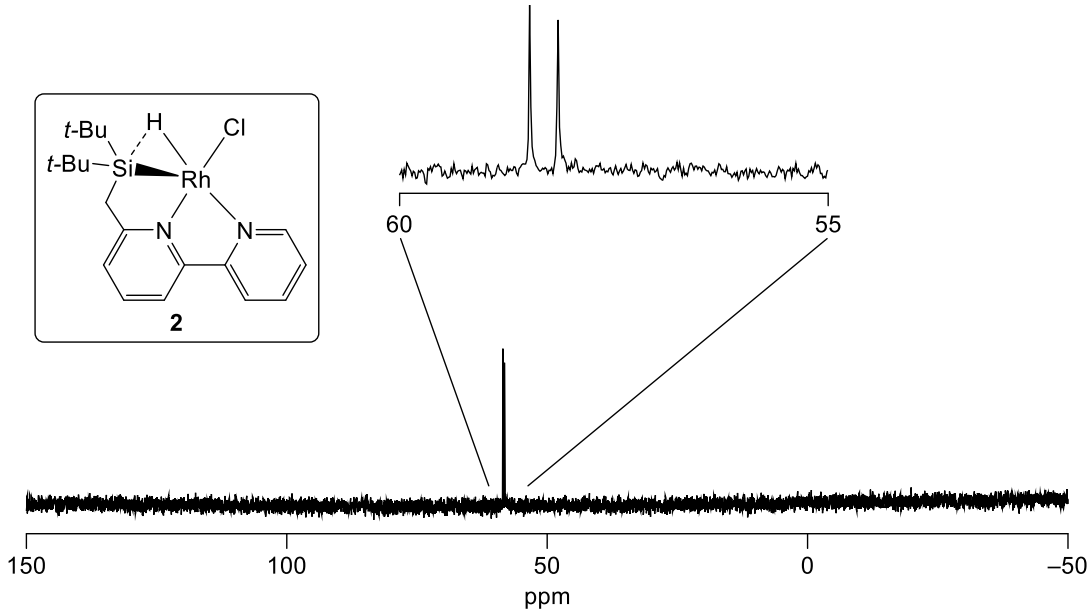


**Fig. S12** $^{29}Si\{^{1}H\}$ NMR spectrum of **2** (79.5 MHz, IG, r.t., THF-$d_8$).

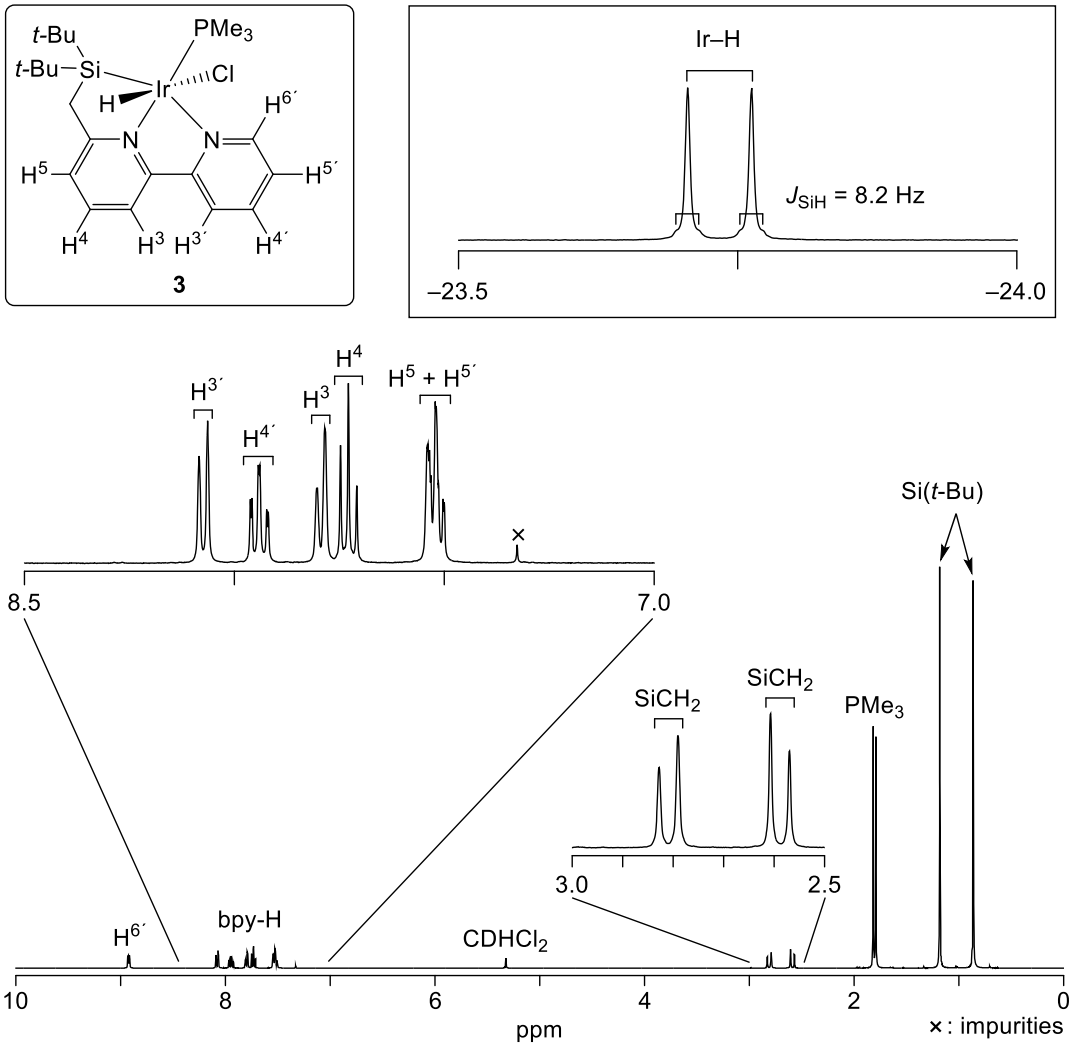


**Fig. S13** $^{1}$H NMR spectrum of Ir(Bpy$^{SiNN}$)(H)($PMe_3$)Cl (**3**) (400 MHz, r.t., $CD_2Cl_2$).

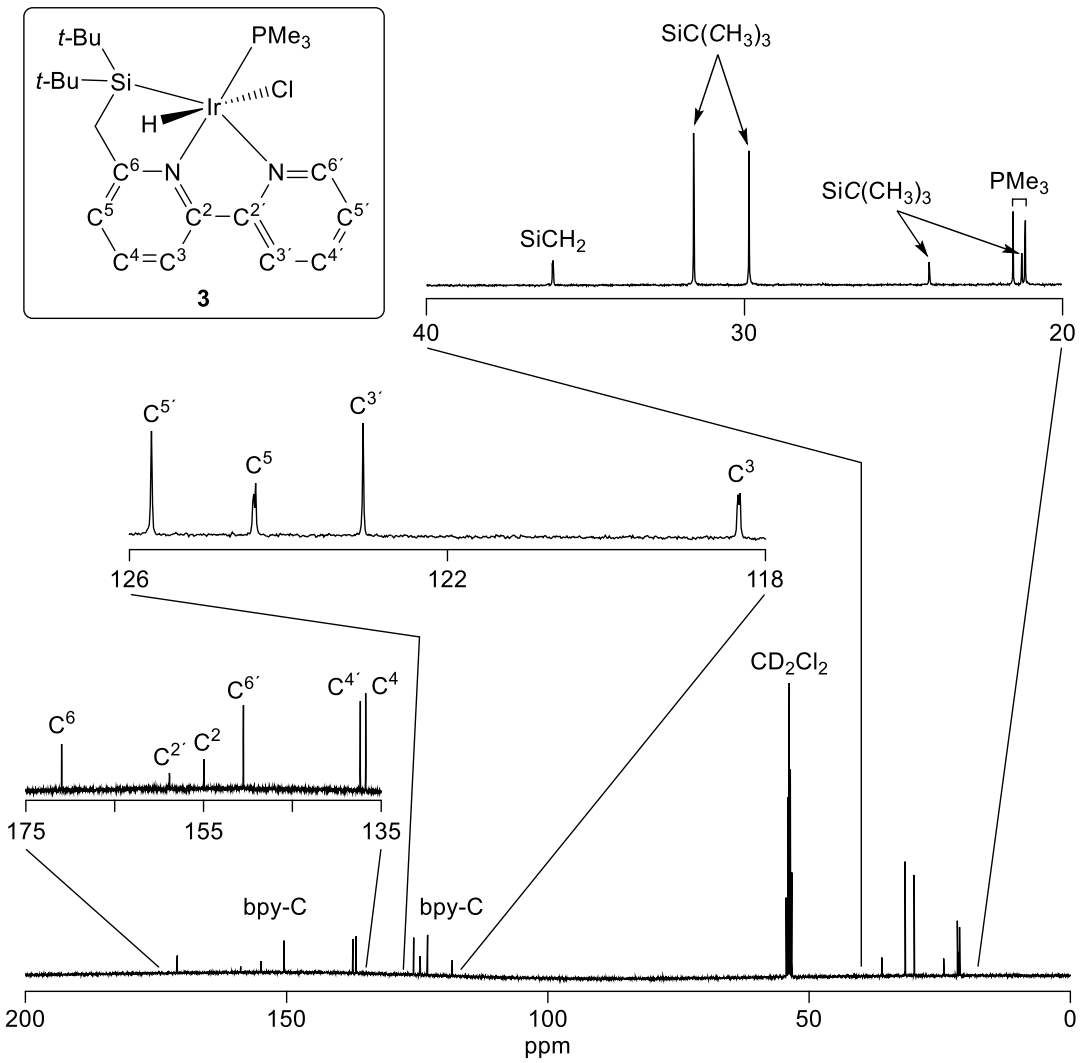


**Fig. S14** $^{13}C\{^{1}H\}$ NMR spectrum of **3** (101 MHz, r.t., $CD_2Cl_2$).

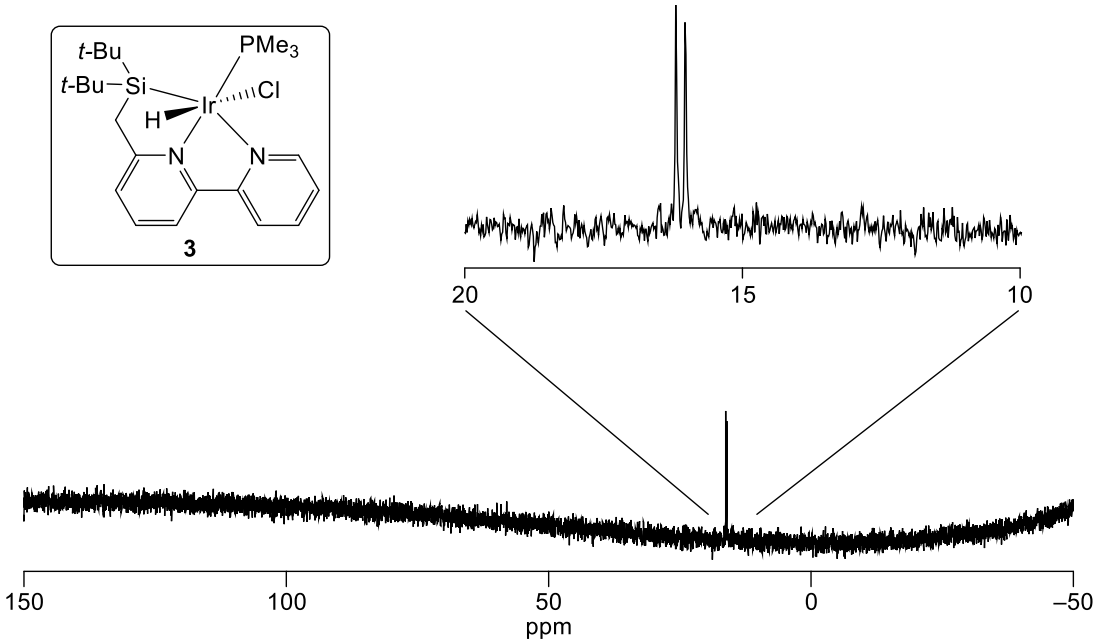


**Fig. S15** $^{29}Si\{^{1}H\}$ NMR spectrum of **3** (79.5 MHz, IG, r.t., $CD_2Cl_2$).

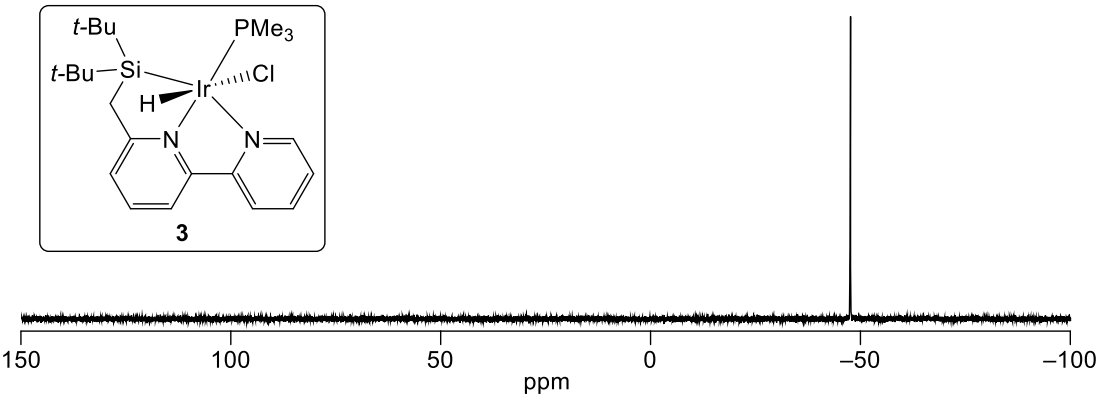


**Fig. S16** $^{31}P\{^{1}H\}$ NMR spectrum of **3** (162 MHz, r.t., $CD_2Cl_2$).

**5. NMR spectra of reaction mixtures of C–H borylation of benzene and benzene-*d*$_6$ with B$_2$pin$_2$ catalysed by complex 1**

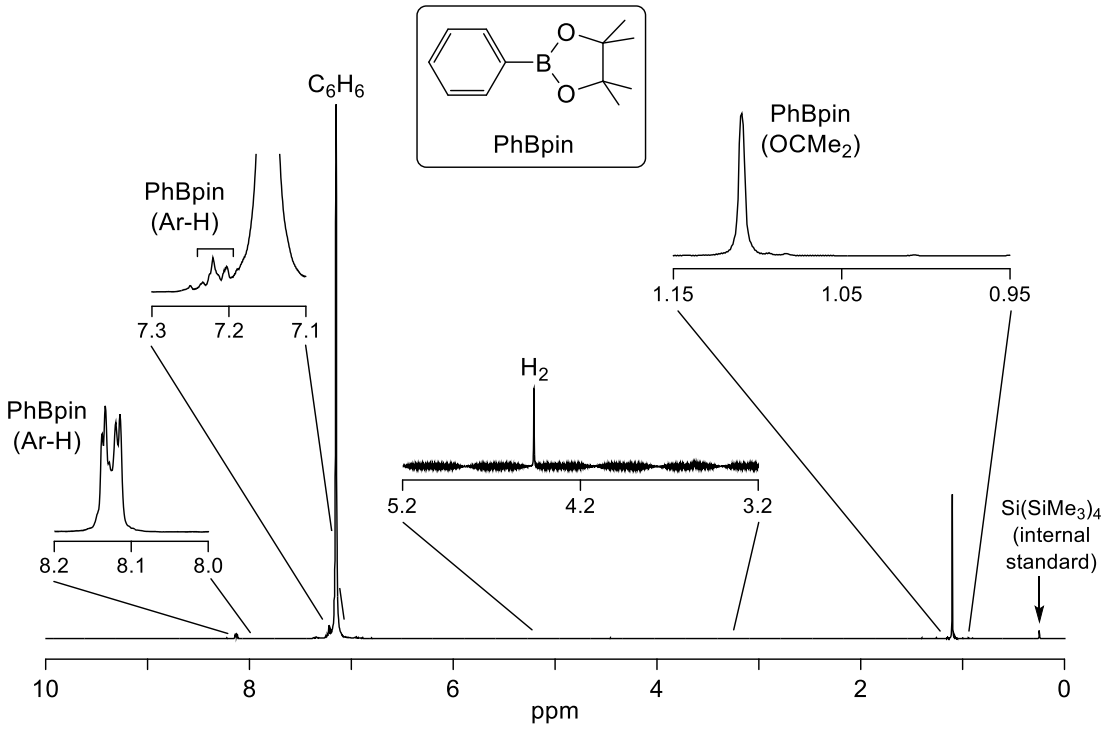


**Fig. S17** $^1$H NMR spectrum of PhBpin in a reaction mixture of $C_6H_6$ with $B_2pin_2$ catalysed by **1** for 24 h at 40 °C [400 MHz, r.t., $C_6H_6$ ($C_6D_6$ in a capillary for external lock)].

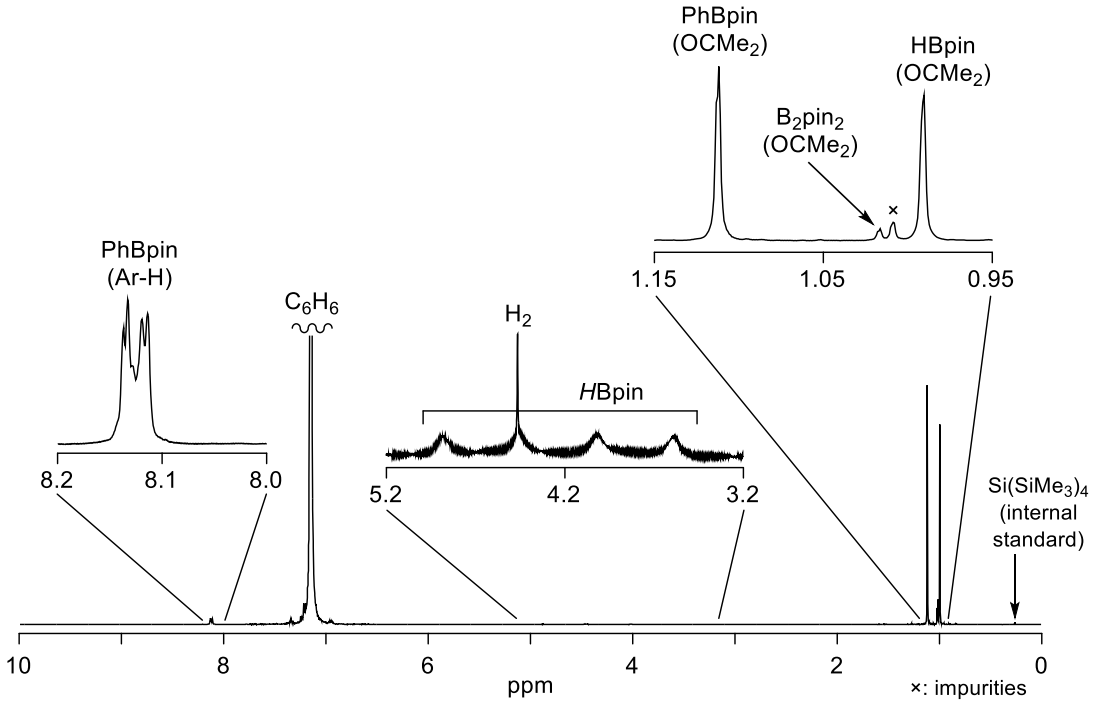


**Fig. S18** $^{1}$H NMR spectrum of a reaction mixture of $C_6H_6$ with $B_2pin_2$ catalysed by **1** after 1 h at 40 °C: observation of HBpin as an intermediate product [400 MHz, r.t., $C_6H_6$ ($C_6D_6$ in a capillary for external lock)].

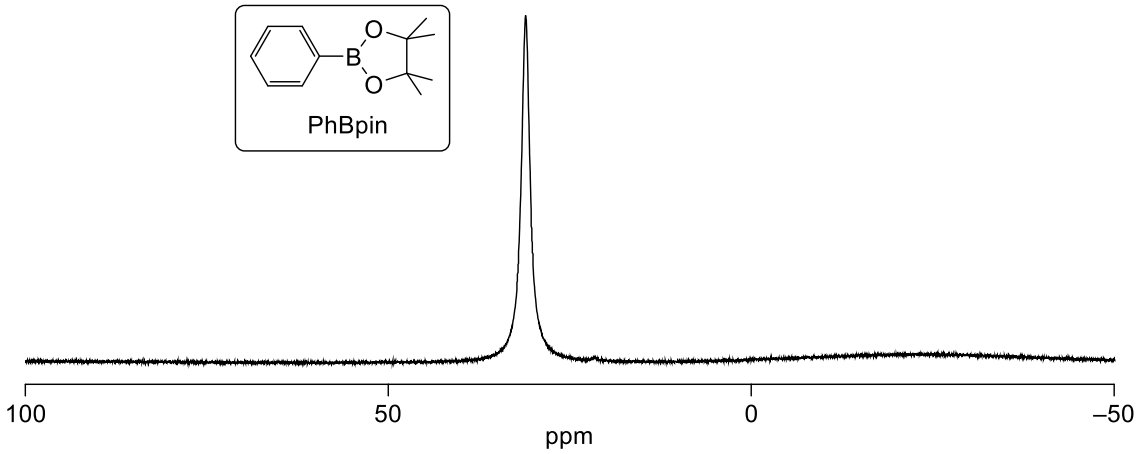


**Fig. S19** $^{11}$B{$^{1}$H} NMR spectrum of PhBpin in a reaction mixture of $C_6H_6$ with $B_2pin_2$ catalysed by **1** after 24 h at 40 °C [128 MHz, r.t., $C_6H_6$ ($C_6D_6$ in a capillary for external lock)].

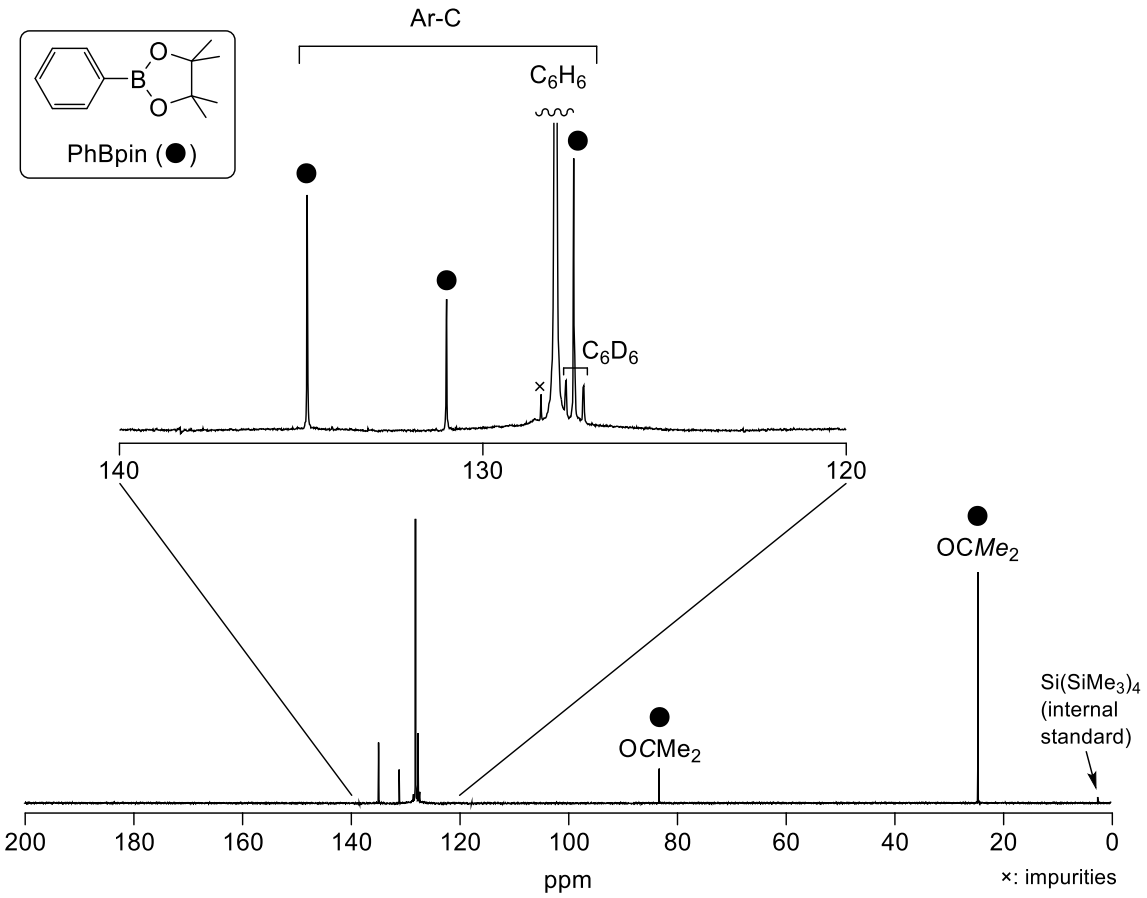


**Fig. S20** $^{13}C\{^{1}H\}$ NMR spectrum of PhBpin in a reaction mixture of $C_6H_6$ with $B_2pin_2$ catalysed by **1** after completion of the C–H borylation [101 MHz, r.t., $C_6H_6$ ($C_6D_6$ in a capillary for external lock)].

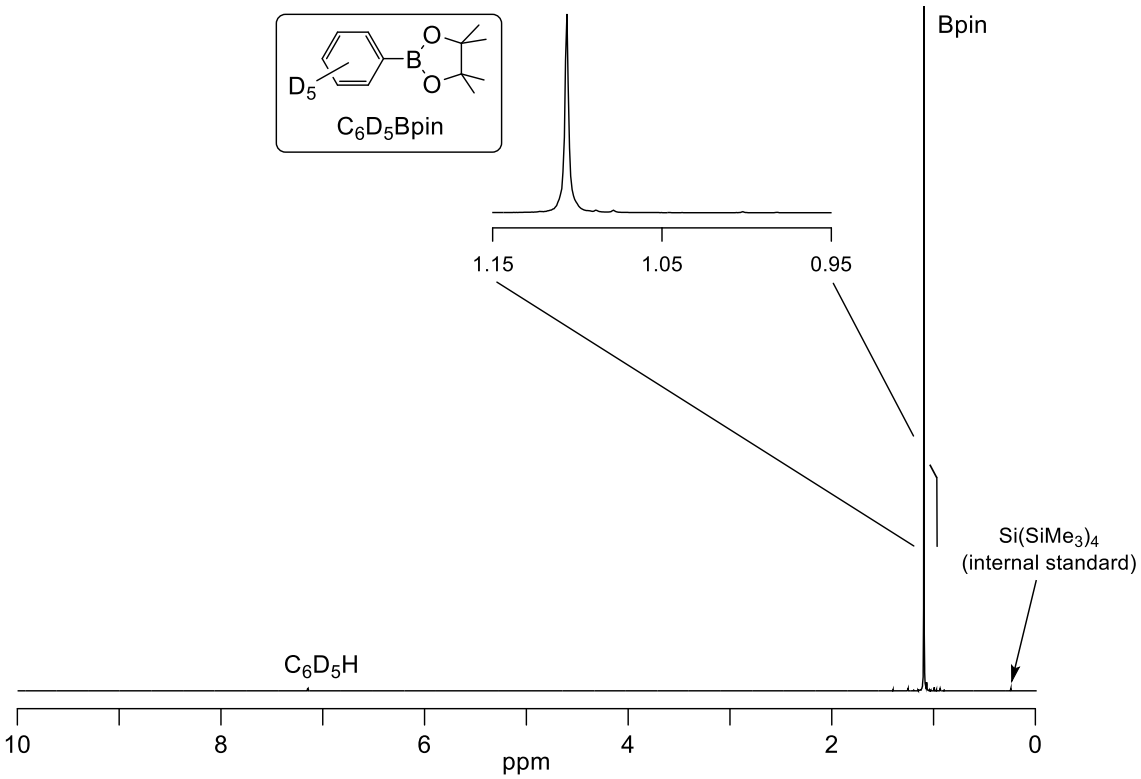


**Fig. S21** $^{1}$H NMR spectrum of $(C_6D_5)$Bpin in a reaction mixture of $C_6D_6$ with $B_2pin_2$ catalysed by **1** after 50 h at 40 °C (400 MHz, r.t., $C_6D_6$).

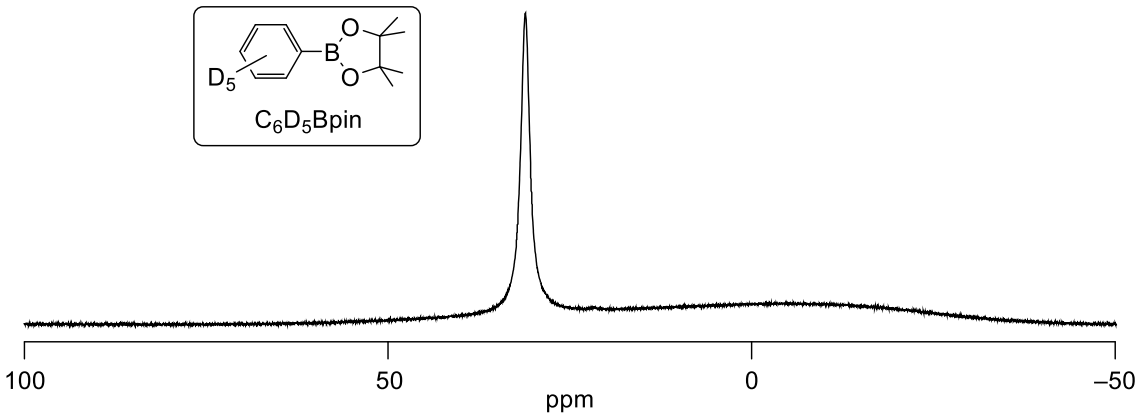


**Fig. S22** $^{11}$B NMR spectrum of $(C_6D_5)$Bpin in a reaction mixture of $C_6D_6$ with $B_2pin_2$ catalysed by **1** after 50 h at 40 °C (128 MHz, r.t., $C_6D_6$).

## 6. NMR spectra of products obtained by C–H borylation of monosubstituted arenes catalysed by 1

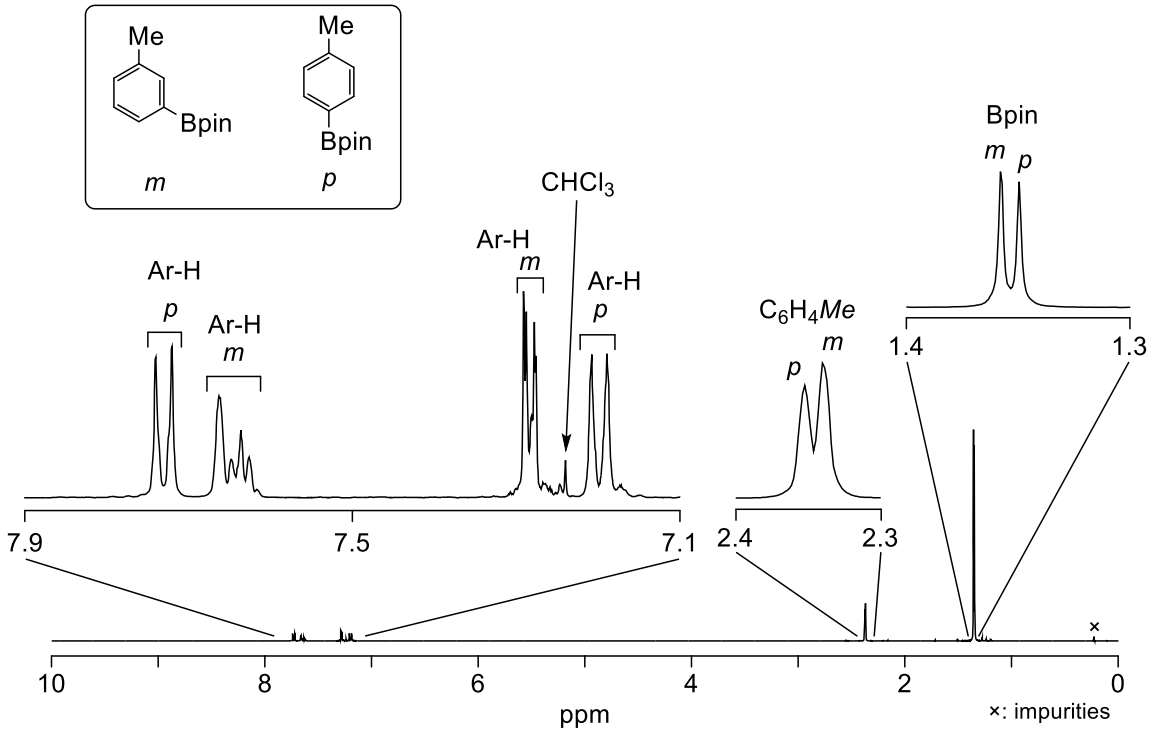


**Fig. S23** $^{1}$H NMR spectrum of an isomeric mixture of the C–H borylation products of toluene (*meta* and *para* isomers) (400 MHz, r.t., $CDCl_3$).

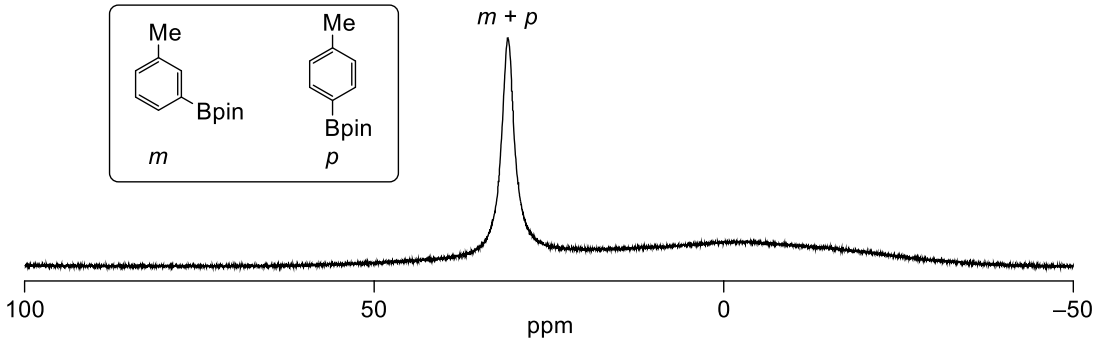


**Fig. S24** $^{11}$B{$^{1}$H} NMR spectrum of an isomeric mixture of the C–H borylation products of toluene (*meta* and *para* isomers) (128 MHz, r.t., $CDCl_3$).

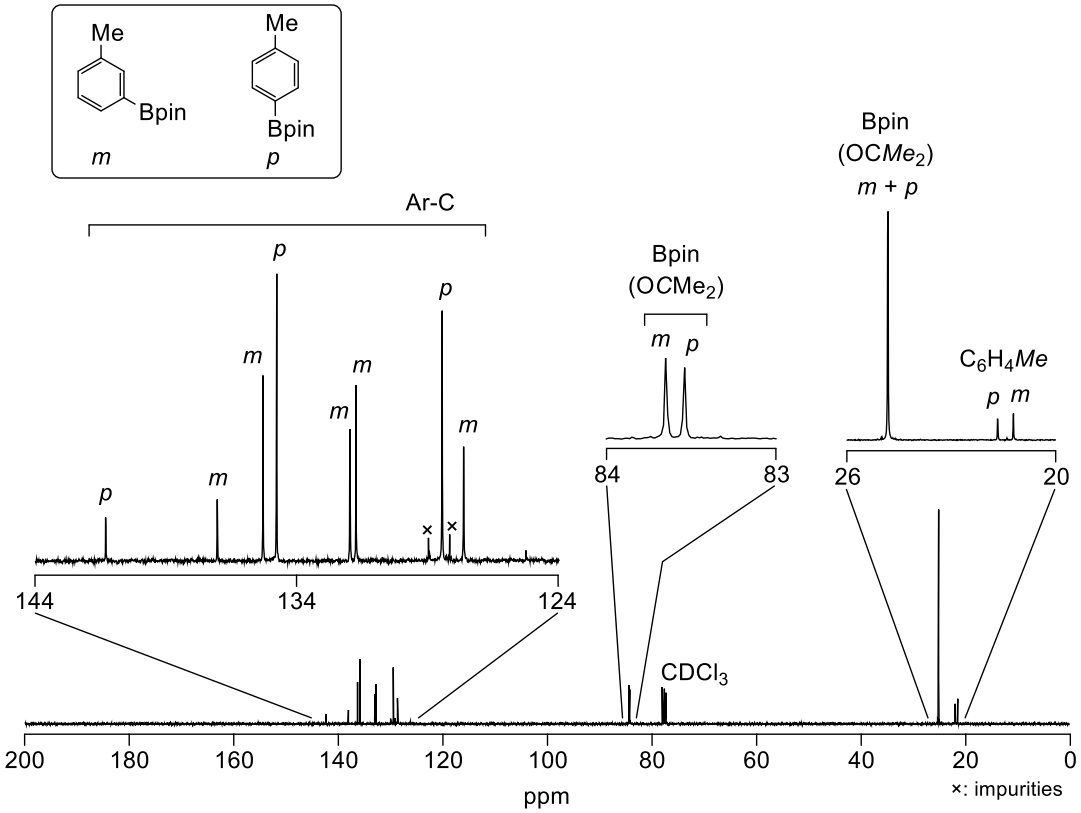


**Fig. S25** $^{13}C\{^{1}H\}$ NMR spectrum of an isomeric mixture of the C–H borylation products of toluene (*meta* and *para* isomers) (101 MHz, r.t., $CDCl_3$).

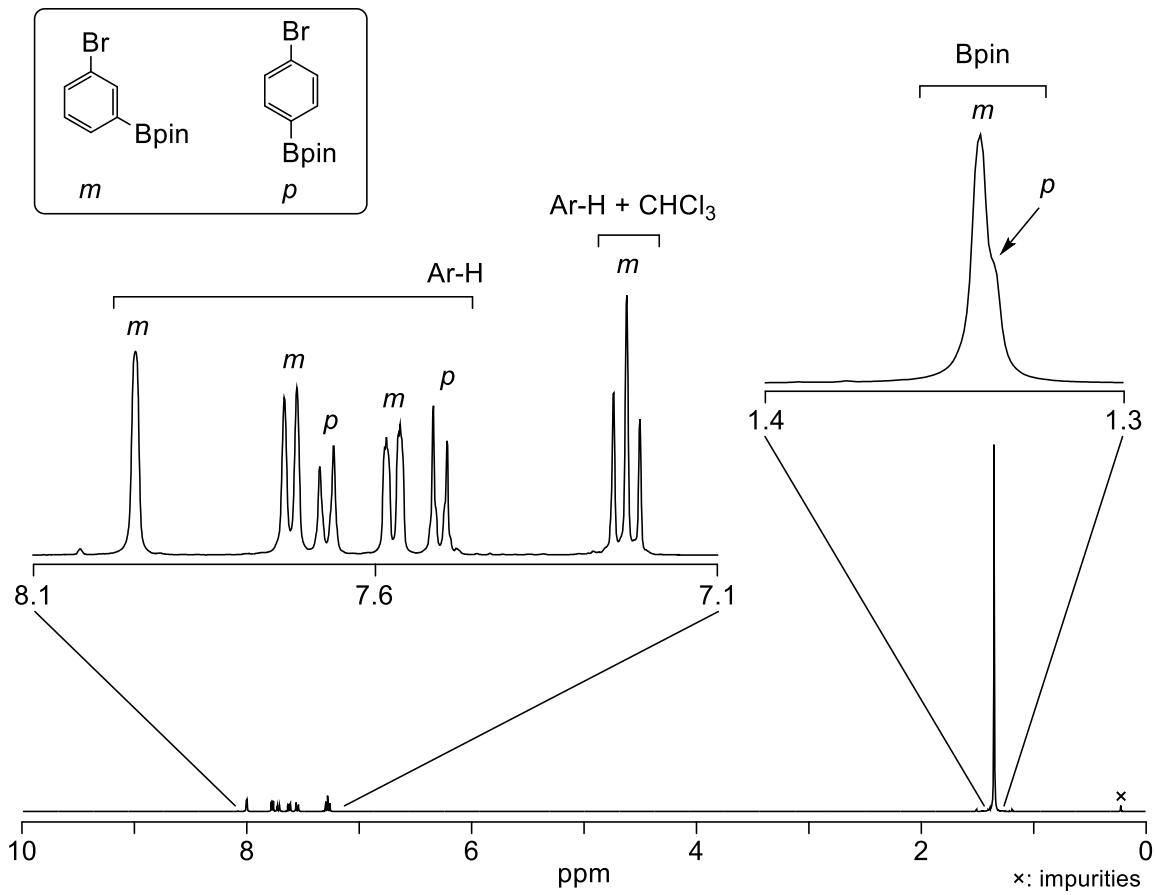


**Fig. S26** $^{1}$H NMR spectrum of an isomeric mixture of the C–H borylation products of bromobenzene (*meta* and *para* isomers) (400 MHz, r.t., $CDCl_3$).

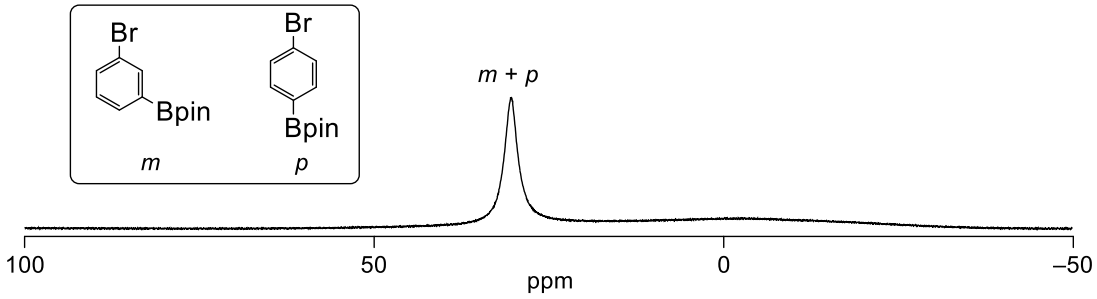


**Fig. S27** $^{11}$B{$^{1}$H} NMR spectrum of an isomeric mixture of the C–H borylation products of bromobenzene (*meta* and *para* isomers) (128 MHz, r.t., $CDCl_3$).

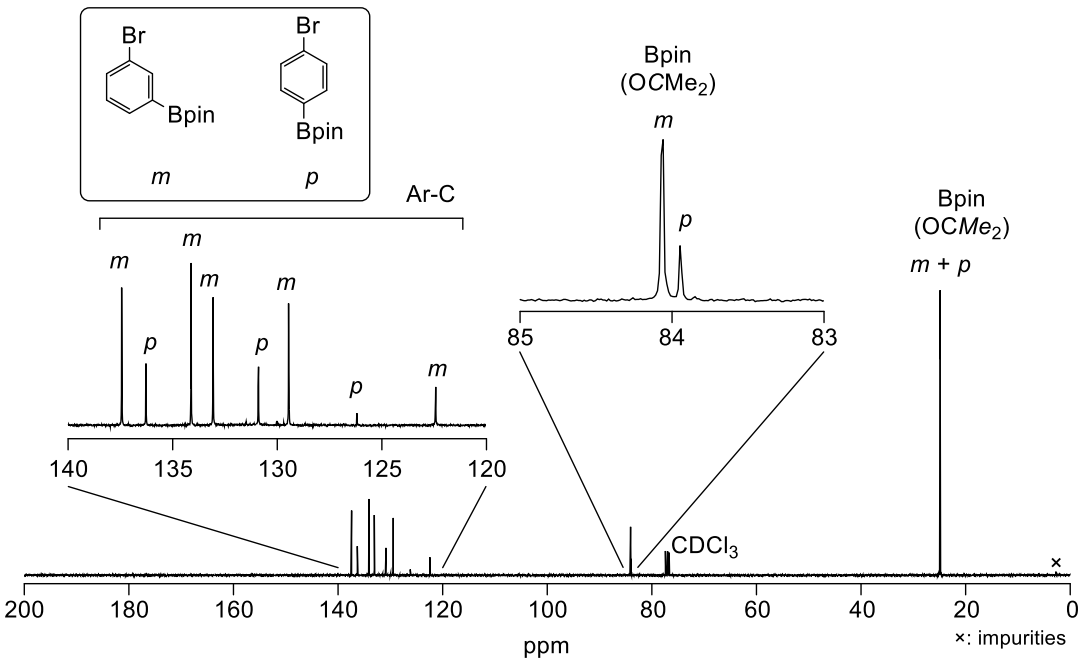


**Fig. S28** $^{13}C\{^{1}H\}$ NMR spectrum of an isomeric mixture of the C–H borylation products of bromobenzene (*meta* and *para* isomers) (101 MHz, r.t., $CDCl_3$).

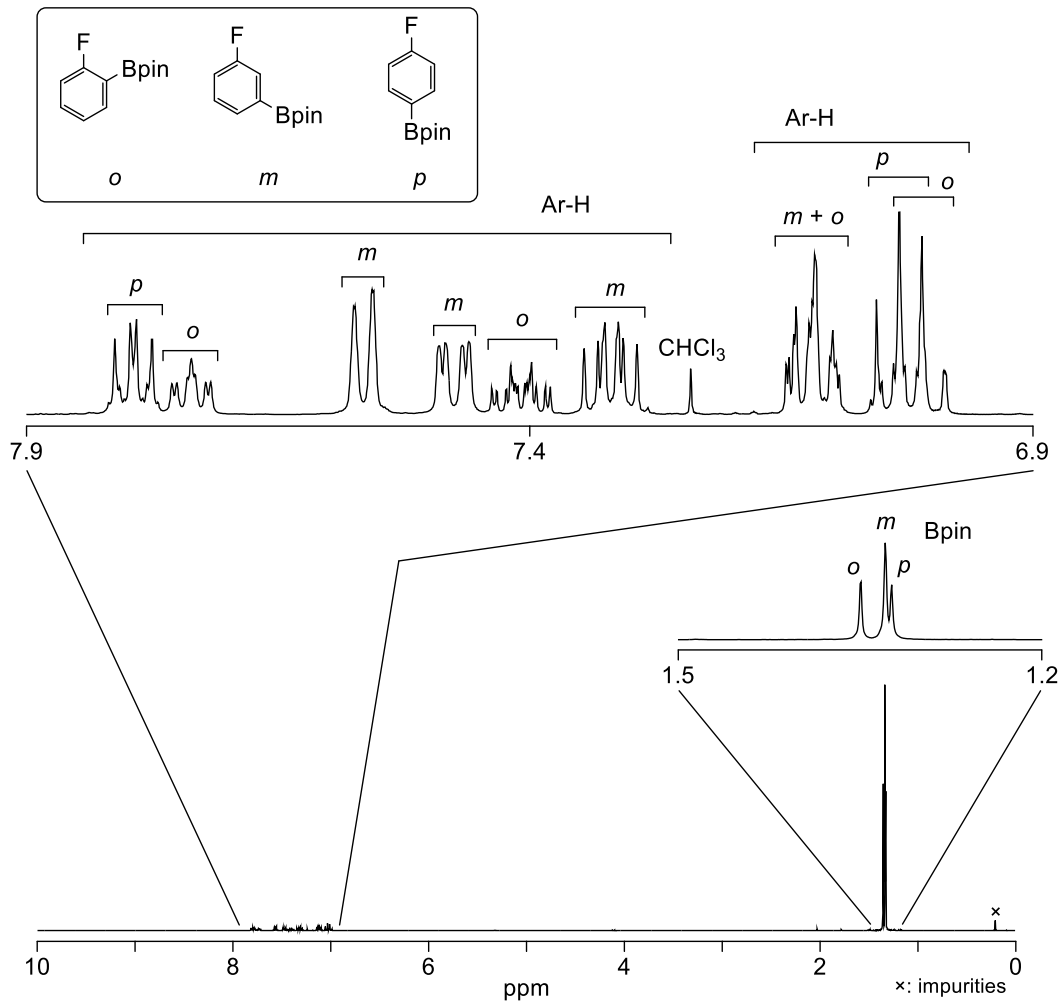


**Fig. S29** $^{1}$H NMR spectrum of an isomeric mixture of the C–H borylation products of fluorobenzene (*ortho*, *meta* and *para* isomers) (400 MHz, r.t., $CDCl_3$).

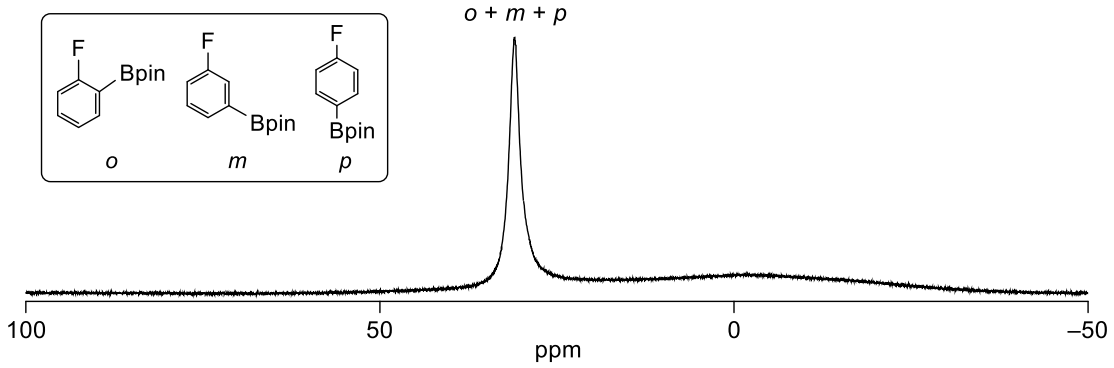


**Fig. S30** $^{11}$B{$^{1}$H} NMR spectrum of an isomeric mixture of the C–H borylation products of fluorobenzene (*ortho*, *meta* and *para* isomers) (128 MHz, r.t., $CDCl_3$).

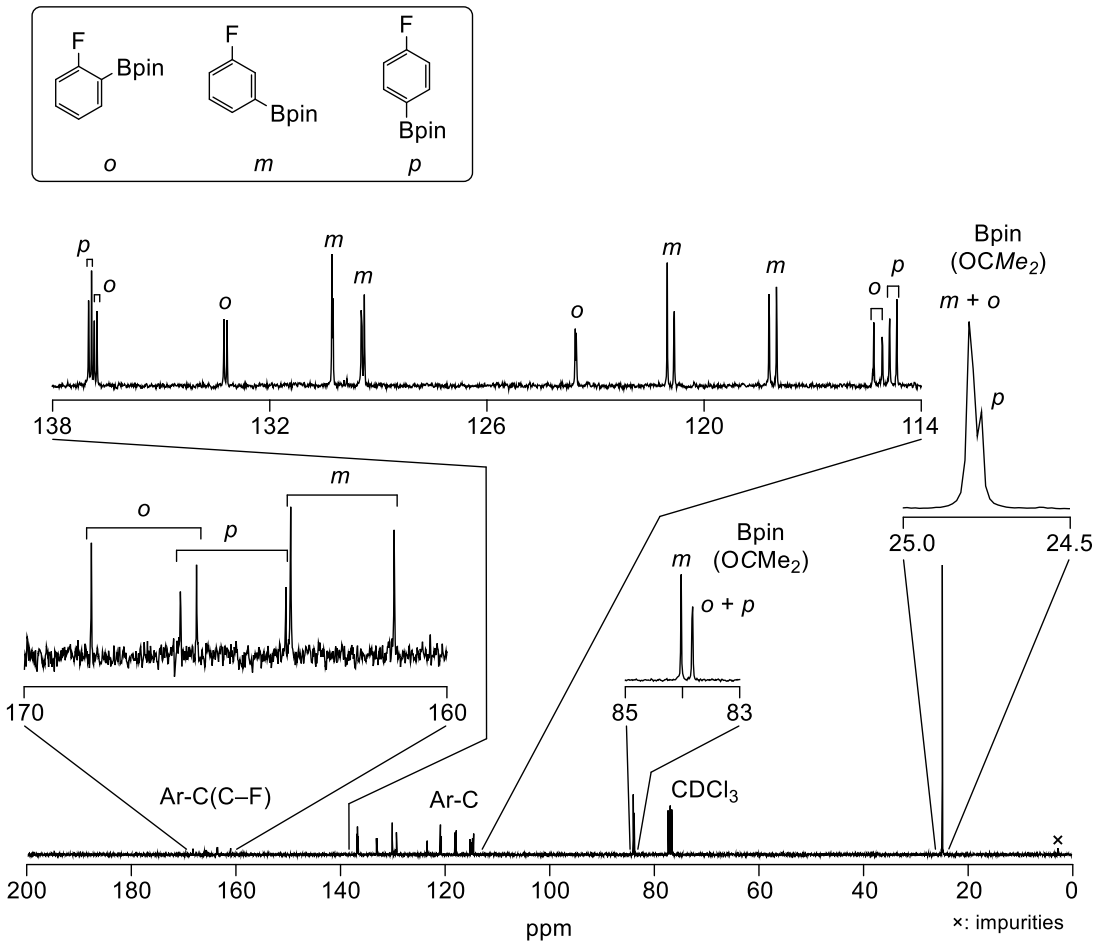


**Fig. S31** $^{13}C\{^{1}H\}$ NMR spectrum of an isomeric mixture of the C–H borylation products of fluorobenzene (*ortho*, *meta* and *para* isomers) (101 MHz, r.t., $CDCl_3$).

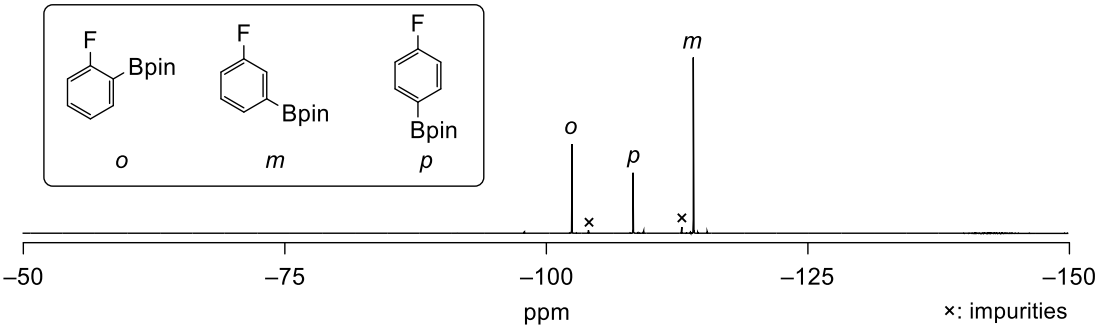


**Fig. S32** $^{19}F\{^{1}H\}$ NMR spectrum of an isomeric mixture of the C–H borylation products of fluorobenzene (*ortho*, *meta* and *para* isomers) (376 MHz, r.t., $CDCl_3$).